INVESTIGATION OF OTA-INDUCED GLOBAL TRANSLATION INHIBITION

by

Semanur Karayılan

B.S., Molecular Biology and Genetics, Bogazici University, 2022

Submitted to the Institute for Graduate Studies in
Science and Engineering in partial fulfillment of
the requirements for the degree of
Master of Science

Graduate Program in Graduate Program in Molecular Biology and Genetics

Boğaziçi University

2025

ACKNOWLEDGEMENTS

First and foremost, I would like to express my sincere gratitude to my supervisor, Assoc. Prof. İbrahim Yaman. I joined MTCRL as an SP student and continued my journey there as a master's student, during which I had the privilege of growing under his mentorship. His openness, trust, and unwavering support created a space where I could develop both scientifically and personally, which solidified my interest in academia.

Next I want to thank my jury members Prof. Arzu Çelik-Fuss and Assoc. Prof. Umut Şahin for their valuable time, thoughtful feedbacks and insightful suggestions. I want to extent my deep gratitude for Prof. Arzu Çelik-Fuss further, for her generous support scientifically and personally, that made me know she was there for anything she can do for me. It is an honor to have her by my side. I want to extent my deepest gratitude to Asst. Prof. Tolga Sütlü. I had the privilege the be one of his students and grateful to him for extending his support and mentorship through hard times and good times alike. I also am grateful to Sütlü Lab members Betül Çakıcı, Elif Çelik, and Serra Özarı for their generous supports and contributions, that helped greatly for the continuation of this thesis. I want to thank Dr. Anıl Şükrü Doğan for his solid support especially in the beginning of this project and encouragements all throughout this journey. I also extent my gratitude to all my KPark residents for their friendship and openness to me. Especially Ulduz Sobhi Afshar and Davod Khalafkhany, for their heartfelt presence, unwavering support, and selfless guidance that always came without hesitation- offering more than just help, but genuine care. I also want to thank İlke Süder, Özen Kaya, and Efe Elbeyli for their steady support, thoughtful guidance, and sincere friendship throughout this journey.

I am truly grateful for being a part of MTCRL and sharing a space with so many wonderful people along the way. In particular, I would like to thank Elif Tula, my first mentor, who taught me how to navigate daily life in the lab, face challenges

with resilience, and pass on knowledge with clarity and care. She is once-in-a-lifetime presence, and I feel incredibly privileged to have had her so close. Her guidance has been foundational, she will always remain one of the most important influences in my life, and I am deeply thankful for the opportunity to learn from her and grow beside her. I also want to thank Kardelen Uzunkaya and Çağla Arslan for their wonderful friendship and irreplacable place in my life. I was truly lucky to have them as fellow master's students, sharing laugh and sadness together. I also extent my gratitude to all internship students for their wonderful presence and dedication to lab, especially Ecenur Türkay, Ömer Faruk Dağılgan, İkbal Şahin, Defne Kara, Naz Özgür, Özge Avcı, Zeliha Tunçdemir and Başak Kurt.

I am truly grateful to my mother, my father and sister for their never ending support. I had the strength and confidence to move forward with their infinite trust and love, which I deeply cherish.

Since the beginning of my Bogazici journey, I have had the privilege of meeting incredible friends with whom I shared countless challenges and unforgettable moments. My 'Joyful Nine' friends Ecenur Türkay, Betül Çakıcı, Bahar Orhan, Elif Karay, Ayşegül Durgun, Egemen Şahin, Ahmetcan Türkoğlu and Berkay Engin. We graduated together, supported each other through internships and SP student days, and remained close even as life scattered us across different corners of the world. Their unwavering presence through every joy, frustration, and hardship has meant everything to me. I feel incredibly fortunate to have each of them in my life, and I cherish and love them all deeply and uniquely.

I am grateful to everyone who taught, encouraged, and supported me throughout this journey. I've met truly kind and generous people, and made incredible friends. My time here will always be cherished as it has shaped me and become an inseparable part of who I am.

This thesis study was supported by The Scientific and Technological Research Council of Turkey (TUBITAK) National Scholarship Program for Master Students TUBITAK-BIDEB 2210/A.

ABSTRACT

INVESTIGATION OF OTA-INDUCED GLOBAL TRANSLATION INHIBITION

Ochratoxin A (OTA) is a widespread nephrotoxic mycotoxin produced by *Aspergillus* and *Penicillium* species, known to exert cytotoxic effects through disruption of cellular homeostasis. One of its widely recognized effects is the suppression of global protein synthesis, which was linked to phosphorylation of eukaryotic initiation factor 2 alpha (eIF2α), though the underlying mechanism remained unresolved. In this MSc thesis, I investigated the role of eIF2α kinases GCN2, PKR, and PERK in OTA-induced stress response across human (HK-2), rat (WB-F344), and mouse (MEF) cell lines using selective chemical inhibitors. Time-course experiments confirmed that OTA induces a robust, time-dependent phosphorylation of eIF2α alongside significant global translation repression in all models. GCN2 inhibition resulted in pronounced reduction in p-eIF2α levels and partial recovery in translation, while effects of PKR and PERK exhibited more cell-type-specific outcomes. Notably, inhibition of ISR kinases exacerbated OTA-induced cytotoxicity with prolonged exposure, underscoring a protective role. I further explored the interplay between eIF2α signaling and the PI3K/Akt/mTOR pathway, a known survival axis also activated by OTA. Results revealed bidirectional crosstalk: eIF2α kinases, especially GCN2, promoted Akt/mTORC1 activation, while PI3K/Akt activity sustained eIF2α phosphorylation. Inhibition of either pathway disrupted this balance and enhanced cytotoxicity. These findings suggest that eIF2α phosphorylation not only inhibits global translation but also drives pro-survival adaptation through interconnected cytoprotective signaling. This study reveals a coordinated OTA stress response dependent on eIF2α phosphorylation and PI3K/Akt/mTOR signaling, offering new insights into adaptation mechanisms and potential therapeutic strategies in toxin-related pathologies.

ÖZET

OTA-GÜDÜMLÜ GLOBAL TRANSLASYON BASKILANMASININ İNCELENMESİ

Ochratoxin A (OTA), *Aspergillus* ve *Penicillium* türleri tarafından üretilen yaygın bir nefrotoksik mikotoksindir ve hücresel dengeyi bozarak sitotoksik etkiler gösterir. Literatürde en yaygın kabul gören etkilerinden biri, küresel protein sentezinin baskılanmasıdır ve bu durum ökaryotik başlatma faktörü 2 alfa (eIF2α) proteininin fosforilasyonu ile ilişkilendirilmiştir; ancak mekanizması net değildir. Bu yüksek lisans tezinde, OTA kaynaklı stres yanıtında eIF2α kinazları GCN2, PKR ve PERK'in rolü, insan (HK-2), sıçan (WB-F344) ve fare (MEF) hücre hatlarında seçici inhibitörler kullanılarak araştırılmıştır. Zaman-bağımlı deneyler, OTA'nın güçlü şekilde eIF2α fosforilasyonu ve translasyon baskılanmasına yol açtığını göstermiştir. GCN2 inhibisyonu tüm hücre hatlarında p-eIF2α seviyelerini azaltmış ve translasyonun kısmen toparlanmasını sağlamıştır; PKR ve PERK'in etkileri ise hücre tipine özgü kalmıştır. ISR kinazlarının inhibisyonu, özellikle GCN2'nin uzun süreli baskılanması, OTA'ya bağlı sitotoksisiteyi artırarak koruyucu rollerini ortaya koymuştur. Ayrıca, OTA ile aktive olduğu bilinen PI3K/Akt/mTOR yolağı ile eIF2α sinyali arasındaki etkileşim incelenmiştir. Bulgular, çift yönlü bir etkileşime işaret etmektedir: eIF2α kinazları (özellikle GCN2), Akt/mTORC1 aktivasyonunu desteklerken; PI3K/Akt aktivitesi de eIF2α fosforilasyonunu sürdürmektedir. Bu dengenin bozulması sitotoksisiteyi artırmıştır. Sonuçlar, eIF2α fosforilasyonunun yalnızca protein sentezini baskılamakla kalmayıp aynı zamanda hücresel hayatta kalmayı destekleyen adaptif bir yanıtı yönettiğini ortaya koymaktadır. Bu çalışma, OTA'ya karşı gelişen koordineli stres yanıtının eIF2α fosforilasyonu ve PI3K/Akt/mTOR sinyal ağlarına dayandığını vurgulamakta ve toksin kaynaklı hastalıklar için yeni tedavi stratejilerine ışık tutabilecek içgörüler sunmaktadır.

TABLE OF CONTENTS

LIST OF FIGURES

LIST OF TABLES

LIST OF SYMBOLS

g	Gram
h	Hour
kDa	Kilodalton
M	Molar
mg	Milligram
mL	Milliliter
mM	Millimolar
mm	Millimeter
ng	Nanogram
°C	Degree Celsius
U	Unit
V	Volt

α	Alpha
β	Beta
μg	Microgram
μL	Microliter
μM	Micromolar

LIST OF ACRONYMS/ABBREVIATIONS

5'cap	5'-7-methylguanosine
A92	GCN2-IN-1
Akt	Protein Kinase B
ATCC	American Type Culture Collection
BEN	Balkan Endemic Nephropathy
BiP	Binding Immunoglobulin Protein
BSA	Bovine Serum Albumin
C16	PKR Inhibitor I
CHX	Cycloheximide
CKD	Chronic Kidney Disease
CO2	Carbon Dioxide
Ctr	Control
CVDK-8	Cell Viability Detection Kit-8
DMEM	Dulbecco's Modified Eagle's Medium
eIF2α	Eukaryotic Initiation Factor 2 Alpha
ER	Endoplasmic Reticulum
FBS	Fetal Bovine Serum
GCN2	General Control Nonderepressible 2
GSH	Glutathionine
GSK'414	GSK2606414
HK-2	Human Kidney 2
HRI	Heme-Regulated eIF2α Kinase
IRES	Internal Ribosome Entry Site
ISR	Integrated Stress Response
MEF	Mouse Embryonic Fibroblast
Met-tRNAiMet	Initiator Methionyl-Transfer RNA
mTORC1	Mammalian Target of Rapamycin Complex 1
mTORC2	Mammalian Target of Rapamycin Complex 2

OTA	Ochratoxin A
PERK	PKR-like Endoplasmic Reticulum Kinase
PI3K/AKT	Phosphoinositide 3-kinase/Protein Kinase B
PKR	Protein Kinase R
PURO	Puromycin
PVDF	Polyvinylidene Fluoride
RPM	Rotation Per Minute
RT	Room Temperature
S6	Ribosomal Protein S6
SDS	Sodium Dodecyl Sulfate
SUnSET	Surface Sensing of Translation
TBS-T	Tris Buffered Saline with Tween-20
TEMED	Tetramethylethylenediamine
TSC2	Tuberous Sclerosis Complex
WB-F344	Rat Liver Progenitor Cell Line

1. INTRODUCTION

1.1. Ochratoxin A (OTA)

Ochratoxin A (OTA), a secondary metabolite, is primarily produced by filamentous fungi belonging to the *Penicillium* and *Aspergillus* genera. It is a chlorinated isocoumarin derivative conjugated to L-phenylalanine via an amide bond (Figure 1.1) (el Khoury and Atoui, 2010). This amphipathic structure, with a lipophilic isocoumarin ring and a hydrophilic amino acid moiety, not only facilitates membrane permeability but also enables OTA to competitively interfere with phenylalanine-utilizing enzymes and causing subsequent disrupting protein synthesis and contributing to its nephrotoxic and carcinogenic effects (Creppy *et al.*, 1983; Gekle *et al.*, 2005).

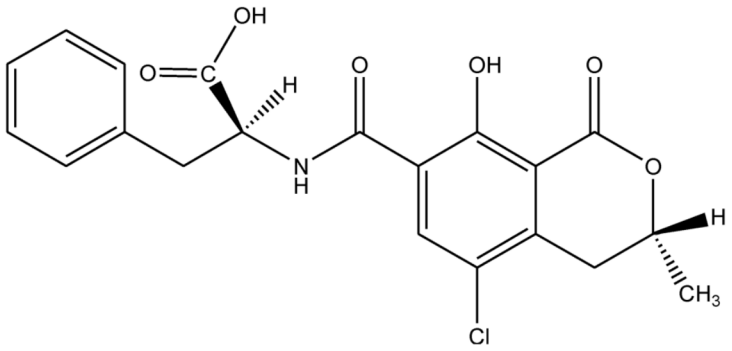

Figure 1.1: The structure of OTA (el Khoury and Atoui, 2010).

OTA is a naturally occurring mycotoxin that poses a significant threat to human and animal health due to its widespread contamination of various agricultural commodities, including cereals, coffee, cocoa, spices, and processed foods like wine, juice, and cheese. OTA is also found in the tissues of animals fed with contaminated fodder, further entering the food chain (Li *et al.*, 2021). Thus, daily OTA exposure is relatively higher than the other contaminants for human and animals. Furthermore,

once exposed, it remains quite stable in the human circulation with a very long half-life around 35 days (800h) (Petzinger and Ziegler, 2000).

Carcinogenic properties of OTA have been established in mice and rats, particularly in the liver and kidneys, alongside various specific toxic effects, including hepatotoxicity, teratogenicity, and immunotoxicity. OTA accumulates in the kidney over time due to reabsorption in the proximal tubules. Also, several studies have reported a correlation between OTA exposure and the development of nephropathies, including renal tumors (el Khoury and Atoui, 2010; Malir *et al.*, 2016). OTA is also strongly implicated as a potential cause of Balkan Endemic Nephropathy (BEN) and related urinary tract tumors in humans. The presence of OTA in blood serum of chronic kidney disease (CKD) patients were reported to be significantly high by several studies (Hmaissia Khlifa *et al.*, 2012; Kosicki *et al.*, 2021; Meucci *et al.*, 2017). As it poses significant health risks, OTA is recognized as a Group 2B carcinogen (possibly carcinogenic to humans) by the International Agency for Research on Cancer (Schrenk *et al.*, 2020). Maximum OTA concentrations allowed on various food commodities are periodically updated and tightly regulated by European Commission (European Commission, 2006). Unfortunately, in third world countries where food storage is particularly poor, OTA regulations are also poor or non-existent.

OTA displays significant species-specific differences in its metabolism and toxicity, which are critical for accurate risk assessment. In rats, elevated levels of glutathione (GSH) conjugates indicate increased bioactivation, potentially contributing to higher nephrotoxicity and genotoxicity. In contrast, OTA does not act as a direct genotoxin in human renal proximal tubular epithelial cells (HK-2); instead, its effects appear to be mediated by oxidative stress. This suggests that OTA undergoes different metabolic processing in human cells. Additionally, the liver contributes to detoxification through the formation of OTAα, whereas the kidney remains more susceptible due to limited detox capacity. The pronounced kidney damage observed in rats, compared to humans or mice, underscores the limitations of rat models in predicting human OTA toxicity (Sorrenti *et al.*, 2013). Therefore, species-specific and cell-type specific analysis in

understanding OTA's cellular and molecular impact is important for accurate interpretation of experimental results and for the development of relevant human health risk assessments.

OTA exerts its toxic effects by interfering with multiple cellular signaling pathways that cause oxidative stress, inflammation, cell cycle arrest, and apoptosis, including PI3K/AKT and MAPK/ERK1-2 pathways to induce survival and apoptosis respectively (Ozcan *et al.*, 2015). One of the critical outcomes of OTA exposure is the inhibition of protein synthesis, often mediated through the phosphorylation of eukaryotic initiation factor 2 alpha (eIF2α), a central regulator of translational control during stress (Creppy *et al.*, 1983).

1.2. Eukaryotic Initiation Factor 2 (eIF2) and Global Translation Initiation

Under normal physiological conditions, eIF2 forms a complex with GTP, and binds to initiator methionyl-transfer RNA (Met-tRNAiMet). This ternary complex, eIF2-GTP-Met-tRNAi, is crucial for providing the initial tRNA to 43S preinitiation complex which is consisted of small ribosomal subunit and various other translational initiation factors. The preinitiation complex binds to the 5'-7-methylguanosine (5' cap) of mRNA and scans the transcript until it finds an initiation codon. Upon binding of Met-tRNAiMet to the initiator codon in the P site of the 40S ribosomal subunit, GTP bound to eIF2 is hydrolyzed and subsequently eIF2-GDP is released. Then, 80S ribosome complex is formed by the addition of 60S ribosomal subunit and elongation of the protein is carried out. For the next round of translation initiation to start, GDP bound to eIF2 must be exchanged for GTP. Guanine exchange factor eIF2B catalyzes this process, enabling the eIF2 reuse for translation initiation (Figure 1.2) (Wek, 2018).

However, when eIF2α subunit is phosphorylated on Ser51 residue, it binds tightly to the eIF2B regulatory subcomplex and prevents the association of eIF2B catalytic subcomplex with eIF2β and eIF2γ subunits required for the nucleotide exchange.

Through this mechanism (Figure 1.3), p-eIF2α acts as a competitive inhibitor, reducing available eIF2B and active eIF2-GTP levels required for pre-initiation complex assembly. As a result, 5'cap mediated global translation is inhibited (Krishnamoorthy *et al.*, 2001).

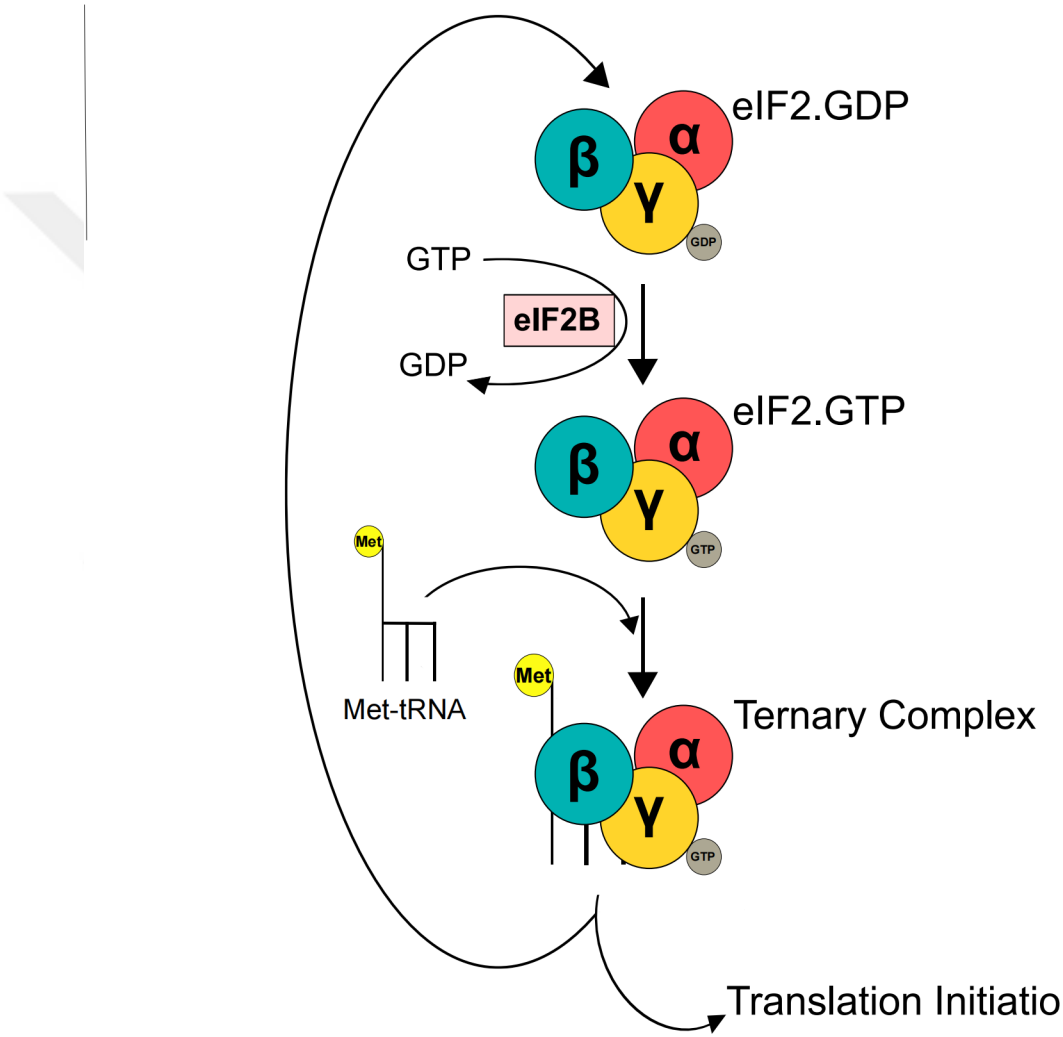

Figure 1.2: Function of eIF2 in translation initiation under normal conditions. eIF2B activates the eIF2–GDP complex by exchanging GDP for GTP. The active eIF2 then forms a ternary complex with Met-tRNA and delivers it to the preinitiation complex. After initiator codon recognition, GTP is hydrolyzed and eIF2 is released; GDP must be exchanged for GTP for the next round [Adapted from (Holcik, 2015)].

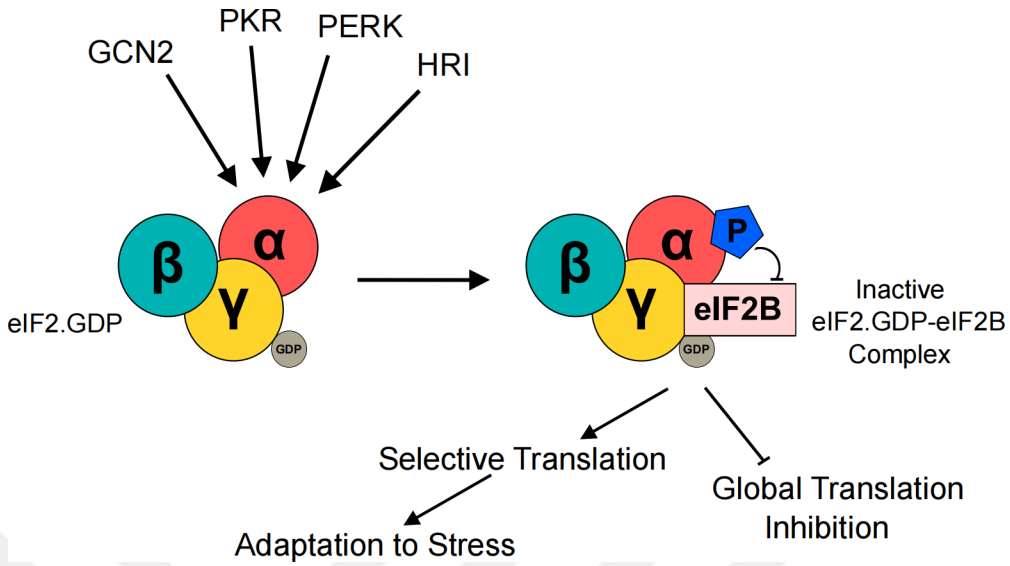

Figure 1.3: The phosphorylation of eIF2α under stress. ISR kinases phosphorylate eIF2α, increasing its affinity for eIF2B and blocking GDP–GTP exchange. This traps eIF2 in an inactive complex, reducing global translation while allowing selective translation of mRNAs that support stress adaptation [Adapted from (Holcik, 2015)].

OTA exposure has been reported to have an inhibitory effect on protein synthesis. However, the experiments conducted on this premise were limited to in vitro experiments, and the OTA dosage used was significantly higher than what would be encountered in physiological conditions (Creppy *et al.*, 1983). Furthermore, OTA was observed to be increasing eIF2α phosphorylation and the involvement of PERK via ER stress were linked in recent studies (Deng *et al.*, 2023; Wang *et al.*, 2022; Yang *et al.*, 2023). On the other hand, there is no direct evidence that the phosphorylation is through specifically PERK and whether other eIF2α kinases have any contribution yet. Thus, the effect of OTA on the eIF2α kinases' activations are yet to be thoroughly discovered.

1.3. ISR Pathway and eIF2α Kinases

In mammals, there are four kinases stimulated by different stress conditions that results in eIF2α phosphorylation which centers Integrated Stress Response (ISR)

pathways. Namely protein kinase R (PKR), PKR-like endoplasmic reticulum kinase (PERK), general control nonderepressible 2 (GCN2) and heme-regulated eIF2α kinase (HRI) are activated mainly by viral infection, endoplasmic reticulum stress, amino acid starvation and heme deficiency, respectively (Pakos-Zebrucka *et al.*, 2016). This regulatory process is integral to diverse cellular functions, including adaptation to environmental challenges, modulation of apoptosis, and regulation of viral infections. Dysregulation of eIF2α phosphorylation is implicated in various pathological conditions, highlighting its significance in cellular homeostasis and disease processes (Holcik, 2015).

GCN2 is highly conserved and widely studied in yeast S. cerevisiae as it is the only kinase of eIF2α in this species. The activation of GCN2 is facilitated through GCN1-GCN20 complex. Upon amino acid starvation, GCN1-GCN20 complex recognizes the uncharged tRNA on A site of elongating ribosomes to facilitate its transfer to GCN2. The complex bound to tRNA physically interacts and cause conformational change on GCN2 that activates its catalytic domain (Marton *et al.*, 1997). The autophosphorylation of the residues Thr-882 and Thr-887 on the activation loop is also required for the full kinase activity (Romano *et al.*, 1998).

PERK is a kinase that is activated upon endoplasmic reticulum (ER) stress, which can be triggered by unfolded proteins. (Teske *et al.*, 2011) Under normal conditions, inactive PERK remains bound to ER chaperone protein BiP (Binding Immuoglobulin Protein or GRP78). Upon ER stress and subsequent accumulation of misfolded proteins, BiP dissociates from PERK to assist their ATP-dependent protein folding. This leads to oligomerization and autophosphorylation of PERK on Thr980, consequently its activation and phosphorylation of eIF2α (Haze *et al.*, 2001).

PKR is the eIF2α kinase that is activated primarily upon double-stranded RNA stress and it responds to viral invasion, endoplasmic reticulum (ER) stress, and interferon signaling (Gal-Ben-Ari *et al.*, 2018). In normal conditions PKR is monomeric; however, viral dsRNA induces conformational change, promoting dimerization which leads to autophosphorylation of Thr-446 and Thr-451 residues on activation loop that

transforms it into an active kinase form resulting in eIF2α phosphorylation and other downstream effects (Romano *et al.*, 1998).

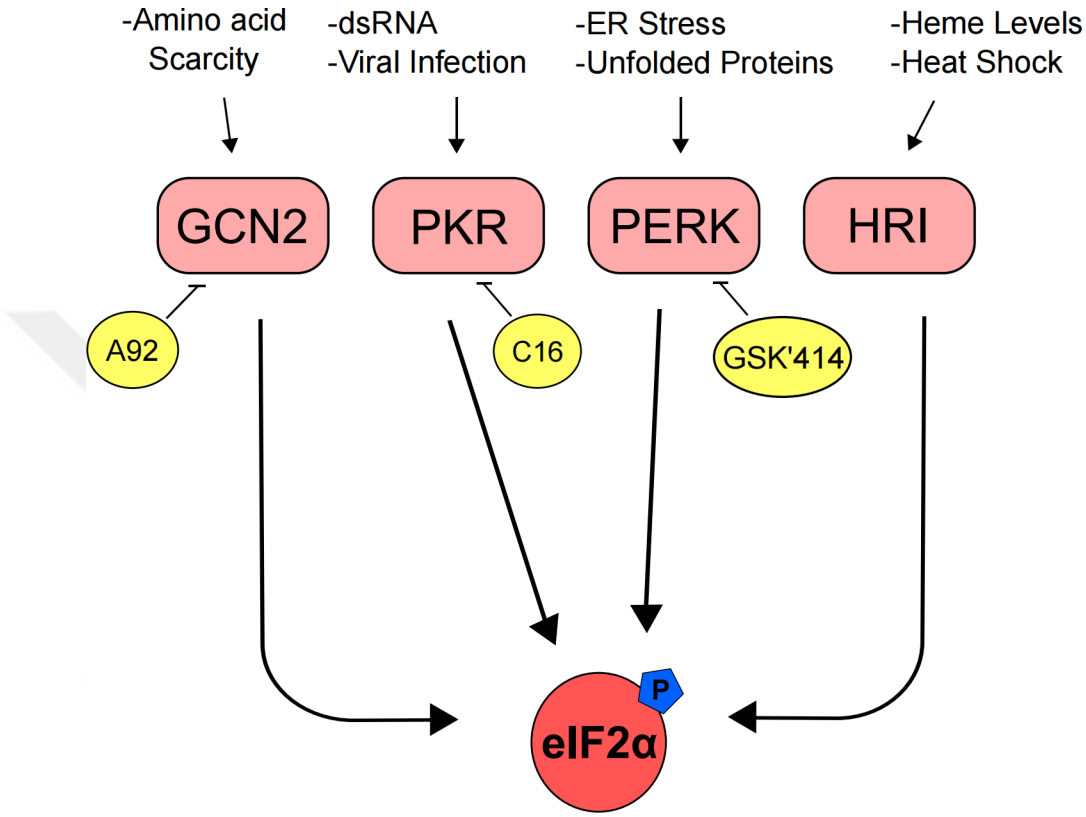

Figure 1.4: Stress-specific activation of eIF2α kinases and their chemical inhibition. GCN2, PKR, PERK, and HRI are activated by distinct cellular stress signals. These kinases phosphorylate the α subunit of eIF2, leading to global translational inhibition (Holcik, 2015). GCN2, PKR and PERK can be individually inhibited by selective chemical inhibitors A92, C12 and GSK'414, respectively (Szaruga *et al.*, 2023).

HRI is one of the eIF2α kinases activated upon heme deficiency conditions and oxidative stress. Inactive HRI contains heme bound to its regulatory domain, which acts as an allosteric inhibitor. When heme levels decrease, HRI dissociates from heme-containing hemoglobin, leading to its autophosphorylation and activation, and consequent eIF2α phosphorylation. This mechanism regulates α- and β-globin levels in red blood cells, limiting their expression by inhibiting global translation under iron/heme

deficiency (Han *et al.*, 2001). Similarly, heat shock and oxidative stress, particularly arsenide exposure, can induce HRI activation, which is crucial for maintaining homeostasis in erythroid cells. While an imbalance in reactive oxygen species can directly phosphorylate and activate HRI leading to eIF2α phosphorylation, heat shock stress requires chaperon proteins hsp90 and hsc70 to regulate HRI activity, which indicates differential activation mechanisms (Lu *et al.*, n.d.; Yerlikaya, 2022)

Most of these kinases can be inhibited selectively via chemical inhibitors in order to prevent kinase specific phosphorylation of eIF2α (Figure 1.4). GCN2-IN-1 (A92) inhibits GCN2 by occupying the ATP-binding site of GCN2 kinase domain, preventing ATP binding and subsequent kinase activation (Brazeau and Rosse, 2014). PERK inhibitor GSK2606414 also binds the ATP-binding pocket of PERK and preventing its autophosphorylation and subsequent activation (Bagratuni *et al.*, 2020). PKR Inhibitor I (C16) disrupts PKR activation by directly binding to the activation loop, preventing autophosphorylation required for the activation (Jammi *et al.*, 2003; Weintraub *et al.*, 2016). Even though the inhibitors are specific to their respective kinases, the intricate ISR mechanisms may cause activation of one eIF2α kinase when another is inhibited, which was studied meticulously in literature (Szaruga *et al.*, 2023).

1.4. PI3K/AKT/mTOR Pathway

Akt (Protein Kinase B) is a central regulator of cell survival, growth, and metabolism, activated downstream of PI3K in response to growth factors and extracellular signals. Once recruited to the plasma membrane, Akt undergoes full activation through dual phosphorylation at Thr308 by PDK1 and Ser473, the latter being mediated by Mammalian Target of Rapamycin Complex 2 (mTORC2). This phosphorylation is essential for Akt's full kinase activity and its regulation of various downstream effectors involved in translation, proliferation, and stress responses (Glaviano *et al.*, 2023).

Among its key downstream targets is the Tuberous Sclerosis Complex (TSC2), a negative regulator of Mammalian Target of Rapamycin Complex 1 (mTORC1). Akt phosphorylates and inactivates TSC2, thereby relieving its suppression on mTORC1 and promoting mTORC1-mediated responses (Inoki *et al.*, 2002). Once activated, mTORC1 phosphorylates effectors such as p70 (S6K1) and 4E-BP1, enhancing cap-dependent translation (Dann and Thomas, 2006). Specifically, mTORC1-mediated phosphorylation of p70 at Thr389 leads to activation of ribosomal protein S6 (S6) via Ser235/Ser236 phosphorylation, which often used as marker for mTORC1 activity (Isotani *et al.*, 1999).

Interestingly, although Akt activation typically drives mTORC1 activity, pharmacological inhibition of mTORC1 by rapamycin has been reported to result in compensatory phosphorylation of Akt at Ser473 in several cancer cell lines, suggesting a feedback survival mechanism (Sun *et al.*, 2005). Moreover, prolonged Akt activation can initiate a negative feedback loop through phosphorylation and subsequent degradation of IRS-1, a scaffold protein essential for upstream PI3K/Akt activation, thereby attenuating its own signaling pathway over time (Yoneyama *et al.*, 2018).

Interestingly, this regulatory complexity extends beyond normal conditions and becomes particularly intricate under stress conditions, such as amino acid deprivation. During amino acid scarcity, global translation rates decrease due to reduced amino acid charged tRNAs and impaired initiation complex formation (Pavlova *et al.*, 2020). However, selective translation of specific mRNAs containing unique regulatory elements, such as internal ribosome entry sites (IRES), allows for efficient translation initiation despite this global translational repression. At the same time, mTORC1 activity can persist through other signaling inputs, such as growth factors or changes in cellular energy status, even in the face of amino acid deprivation. This activation acts as a compensatory mechanism, counteracting decreased global translation and ensuring the selective translation of stress-responsive mRNAs essential for survival (Torrence *et al.*, 2021). The delicate balance between reduced global translation and sustained

mTORC1 activity underscores the cell's remarkable ability to prioritize specific translation and adapt to amino acid deprivation.

eIF2α phosphorylation (p-eIF2α), activated by GCN2 and PERK, has been shown to protect immortalized and tumor cells from oxidative damage. In p-eIF2α-proficient cells, Akt is activated via an ATF4-independent pathway, and mTORC1 inhibition by rapamycin further promotes Akt phosphorylation at the S473 residue, enhancing cell survival. In contrast, p-eIF2α-deficient cells exhibit reduced Akt activation, making them more susceptible to death under oxidative stress. Although low Akt activation in these cells has a pro-apoptotic effect, mTORC1 inhibition still increases Akt phosphorylation, exacerbating the apoptotic response (Rajesh *et al.*, 2015).

OTA is known to be increasing Akt phosphorylation and mTORC1 activation in time- and dose- dependent manner (Figure 1.5), promoting survival under stress conditions. It also was shown that the inhibition of PI3K/Akt pathway with wortmannin decreased cell viability under OTA exposure in HK2 cells (Ozcan *et al.*, 2015). Even though OTA was also reported to be inducing eIF2α phosphorylation like these pathways (Deng *et al.*, 2023; Wang *et al.*, 2022), potential cross-talk was not studied in literature.

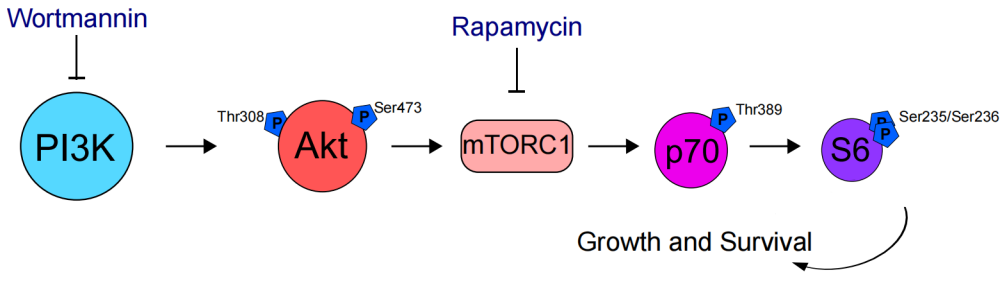

Figure 1.5: OTA-induced PI3K/Akt/mTOR pathway. The pathway can be inhibited by selective inhibitors targeting PI3K and mTORC1 activation by wortmannin and rapamycin, respectively (Akpinar *et al.*, 2019; Ozcan *et al.*, 2015).

2. HYPOTHESIS AND PURPOSE

Ochratoxin A (OTA) is a potent mycotoxin with well-established nephrotoxic and carcinogenic effects. One of its critical cellular impacts is the disruption of protein synthesis (Creppy *et al.*, 1983), often regulated by phosphorylation of the translation initiation factor eIF2α, a key event in the Integrated Stress Response (ISR). However, the specific kinase responsible for eIF2α phosphorylation under OTA exposure, among PERK, PKR, GCN2, or HRI, remains elusive. While eIF2α phosphorylation broadly represses translation, the contribution of individual ISR kinases to this effect under OTA stress remains to be clarified. In parallel, OTA is known to activate key pro-survival pathways including PI3K/Akt/mTOR, which regulate cell growth, metabolism, and stress adaptation (Ozcan *et al.*, 2015). However, the cross-talk between these signaling pathways and ISR-mediated translational control has not been systematically examined. It remains unclear whether these responses occur independently or form a coordinated cellular strategy to counteract OTA-induced stress.

We hypothesize that OTA induces global translational repression primarily through eIF2α phosphorylation mediated by one or more ISR kinase. Furthermore, we propose that OTA-induced activation of the PI3K/Akt/mTOR pathway may intersect with or modulate ISR signaling, and that the balance between these pathways determines the cellular outcome under OTA-induced stress. Identifying the kinase(s) involved and characterizing these mechanisms across species will enhance our understanding of OTA toxicity, and guide therapeutic targeting of ISR signaling.

Based on this hypothesis, the specific aims of the project are:

i) To investigate the effects of OTA on eIF2α phosphorylation and global translation rate in HK2, WBF344, and MEF cell lines.

ii) To determine the impact of eIF2α kinase inhibition on OTA-induced changes in eIF2α phosphorylation, global translation rate, and cell viability.

iii) To investigate the interaction between PI3K/Akt/mTOR signaling and eIF2α phosphorylation under OTA exposure.

In order to achieve those aims;

- The effect of OTA on eIF2α phosphorylation and global translation rate was investigated in HK2, WBF344, and MEF cell lines.

- The impact of eIF2α kinase inhibition on eIF2α phosphorylation and global translation rate under OTA exposure was assessed.

- The effects of eIF2α kinase inhibition on cell viability under OTA exposure were evaluated.

- The effects of eIF2α kinase inhibition on key components of PI3K/Akt/mTOR pathway under OTA exposure were investigated.

- The effects of PI3K/Akt inhibition via Wortmannin on eIF2α phosphorylation and global translation rate under OTA exposure were examined.

- The effects of mTOR inhibition via Rapamycin on eIF2α phosphorylation and global translation rate under OTA exposure were investigated.

3. MATERIALS

3.1. Cell Culture

Human Kidney 2 (HK-2) cells were purchased form American Type Culture Collection (ATCC) (Manassas, USA). Rat liver progenitor cells (WB-F344) were kindly provided by Assoc. Prof. Mehmet Akıf KILIC from Akdeniz University, Antalya, Turkey. Mouse embryonic fibroblast cells (MEF) were kindly provided by Prof. Devrim GOZUACIK from Koc University, Istanbul, Turkey. Cell culture solutions used in this thesis listed in Table 3.1. Chemicals used in cell culture experiments listed in Table 3.2.

Table 3.1: Cell Culture Solutions.

Solution	**Supplier**
Dulbecco's Modified Eagle Medium: Nutrient Mixture F-12 (DMEM / F-12)	11320-074, Gibco, USA
Fetal Bovine Serum (FBS)	A5256701, Gibco, USA
Penicillin/Streptomycin (100X)	Gibco, USA
L-Glutamine 200 mM	P04-80100, Gibco, USA
MEM NEAA (100X)	11140-035, Gibco, USA
Trypsin-EDTA (0.05%)	Gibco, USA
DMSO	BioFroxx, Germany
PBS	MP Biomedicals, LLC, France

Table 3.2: Chemicals Used in Cell Culture.

Chemical	**Supplier**
Ochratoxin-A	O1877, Sigma-Aldrich, USA
Wortmannin	9951, Sigma-Aldrich, USA
Rapamycin	53123-88-9, Sigma-Aldrich, USA
GCN2-IN-1 (A92)	HY-100877, MedChemExpress, USA
PKR inhibitor C16	527450-5MG, Sigma-Aldrich, USA
PERK Inhibitor I (GSK2606414)	HY-18072, MedChemExpress, USA
Puromycin	Sigma-Aldrich, USA
Cycloheximide	Sigma-Aldrich, USA

3.2. Kits and General Chemicals

The kits and general chemicals used in this study are listed in Table 3.3 and Table 3.4, respectively.

Table 3.3: Kits Used in This Study.

Kit	**Supplier**
BCA Protein Assay Kit	Pierce, USA
NutriCulture Cell Viability Detection Kit-8 (CVDK8)	EcoTech, Turkey
Clarity Western ECL Substrate	Bio-Rad, USA
PageRuler Prestained Protein Ladder	Thermo Scientific, USA
Prime-Step™ Prestained Broad Range Protein Ladder	BioLegend, USA

Table 3.4: General Chemicals Used in This Study.

Chemicals	**Supplier**
2-Mercaptoethanol	Sigma-Aldrich, USA
2-Propanol	Sigma-Aldrich, USA
Absolute Ethanol	Merck, USA
Acrylamide/Bis-acrylamide, 40% solution	BioFroxx, Germany
Ammonium Persulfate	AppliChem, Germany
Ampicillin	Roche, Switzerland
Aprotinin Protease Inhibitor	ThermoFisher Scientific, USA

Table 3.4: General Chemicals Used in This Study (cont.)

Chemicals	**Supplier**
Bovine Serum Albumin (BSA)	BioFroxx, Germany
Bromophenol Blue	Merck, USA
EDTA	AppliChem, Germany
Ethanol	Merck, USA
Ethidium Bromide	Sigma-Aldrich, USA
Glycerol	Sigma-Aldrich, USA
Glycine	AppliChem, Germany
Leupeptin Protease Inhibitor	ThermoFisher Scientific, USA
Magnesium Chloride ($MgCl_2$)	Sigma-Aldrich, USA
Methanol	VWR Chemicals, USA
NP-40	Roche, Switzerland
Pepstatin A Protease Inhibitor	ThermoFisher Scientific, USA
Potassium Acetate (KAc)	AppliChem, Germany
Skim Milk Powder	Havancızade, Turkey
Sodium Chloride (NaCl)	Fisher Scientific, USA
Sodium Deoxycholate	Sigma-Aldrich, USA

Table 3.4: General Chemicals Used in This Study (cont.)

Chemicals	**Supplier**
Sodium Hydroxide (NaOH)	Sigma-Aldrich, USA
Sucrose	Sigma-Aldrich, USA
TEMED	Sigma-Aldrich, USA
Tris-Base	AppliChem, Germany
Tris-HCl	AppliChem, Germany
Tween-20	Sigma-Aldrich, USA

3.3. Buffers, Solutions and Antibodies

Buffers and solutions used in Western blot are listed in Table 3.5. Antibodies used are listed in Table 3.6.

Table 3.5: Buffers and Solutions Used in Western Blot Experiments.

Buffer/Solution	**Content**
RIPA Buffer	150 mM NaCl, 1% NP40, 0.5% Sodium deoxycholate, 0.1% SDS, 50 mM Tris pH 7.4, Protease Inhibitors, Phosphatase Inhibitors, 1 mM PMSF
Protease Inhibitors (in RIPA)	0.1 µg/ml Pepstatin A, 0.1 µg/ml Leupeptin, 10 µg/ml Aprotinin
Phosphatase Inhibitors (in RIPA)	5 mM Sodium fluoride (NaF), 2 mM Sodium pyrophosphate ($Na_4P_2O_7$), 2 mM β-Glycerophosphate, 2 mM Sodium orthovanadate (Na_3VO_4)
4X Protein Loading Dye	200 mM Tris-HCl pH 6.8, 8% (w/v) SDS, 40% (w/v) Glycerol, 4% (v/v) β-mercaptoethanol, 50 mM EDTA, 0.08% (w/v) Bromophenol Blue
10% Resolving Gel	375 mM Tris-HCl pH 8.8, 0.1% (w/v) SDS, Acrylamide:Bisacrylamide (12% w/v), 0.05% (w/v) APS, 0.005% (w/v) TEMED

Table 3.5: Buffers and Solutions Used in Western Blot Experiments (cont.)

Buffer/Solution	**Content**
4% Stacking Gel	125 mM Tris-HCl pH 6.8, 0.1% (w/v) SDS, Acrylamide:Bisacrylamide (4% w/v), 0.05% (w/v) APS, 0.0075% (w/v) TEMED
10X SDS Running Buffer	375 mM Tris-HCl pH 8.8, 0.1% (w/v) SDS, Acrylamide:Bisacrylamide (10% w/v), 0.05% (w/v) APS, 0.005% (w/v) TEMED
1X Tris Buffered Saline with Tween-20 (TBS-T)	50 mM Tris-HCl pH 7.4, 150 mM NaCl, 0.1% Tween-20
Western Blot Blocking Solution	5% (w/v) skim milk powder dissolved in TBS-T
1st Antibody Solution	5% (w/v) BSA dissolved in TBS-T
2nd Antibody Solution	5% (w/v) skim milk dissolved in TBS-T
1X Wet Transfer Buffer	48 mM Tris-Base, 39 mM Glycine, 10% (v/v) Absolute EtOH or Methanol

Table 3.6: Antibodies Used in Western Blot Experiments.

Antibody	**Company**	**Dilution**	**Host**
anti-Puromycin	Merck, USA	1:1000	Mouse
eIF2α	Cell Signalling Technologies, USA	1:1000	Rabbit
GAPDH	Cell Signalling Technologies, USA	1:1000	Rabbit
p70	Cell Signalling Technologies, USA	1:1000	Rabbit
phospho-Akt (Ser473)	Cell Signalling Technologies, USA	1:1000	Rabbit
phospho-eIF2α (Ser51)	Cell Signalling Technologies, USA	1:1000	Rabbit
phospho-ribosomal protein S6	Cell Signalling Technologies, USA	1:1000	Rabbit
phospho-p70 (Thr389)	Cell Signalling Technologies, USA	1:1000	Rabbit
β-actin	Cell Signalling Technologies, USA	1:1000	Rabbit
Rabbit IgG, HRP	Cell Signalling Technologies, USA	1:10000	Goat
Mouse IgG, HRP	Cell Signalling Technologies, USA	1:10000	Horse

3.4. Equipments

Equipments used in this study are listed in Table 3.8.

Table 3.7: Equipment used in this study.

Equipment	**Supplier**
Autoclave	Model ASB260T Astell Swiftclave, UK
Balance	AY123, Sartorius, Germany
Centrifuge	Allegra X-22, Beckman Coulter, USA; Allegra X-30 R, Beckman Coulter, USA
CO_2 Incubator	Steri Cycle i60, Thermo Fisher Scientific, USA
Cold Room	Birikim Elektrik Soğutma, Turkey
Deep Freezer ($-150\,^{\circ}C$)	Sanyo MDF-1156, UK; Thermo Scientific, USA
Deep Freezer ($-20\,^{\circ}C$)	Uğur, UFR 370 SD, Turkey
Deep Freezer ($-80\,^{\circ}C$)	Sanyo Ultra Low, UK; Thermo Scientific, USA
Documentation System	Gel Doc XR System, Bio-Doc, Italy; G-BOX Chemi XX6, Syngene, UK
Hemocytometer	ISOLAB, Neubauer, 075.03.001, Germany

Table 3.7: General Equipment used in this study (cont.)

Equipment	**Supplier**
Ice Machine	Scotsman Inc., Italy
Magnetic Stirrer	MS-H-S, Dragonlab, China
Microcentrifuge	VWR CT15RE, Japan
Microliter Pipettes	Axygen, USA
Microplate Reader	680, Bio-Rad, USA
Microscopes	Inverted Microscope, Nikon Eclipse TS100, Netherlands; Fluorescence Microscope, Zeiss Observer.Z1, Germany
Microspin	VWR Galaxy Ministar, USA
Oven	Gallenkamp 300, UK
pH Meter	Mettler Toledo, USA
Pipettor	Brandtech Accu-jet, USA
Power Supply	Power Pac Universal, Bio-Rad, USA
Refrigerator (4 °C)	Uğur, USS 300 DTK, Turkey
SDS-PAGE Transfer System	Bio-Rad, USA
Software	ImageJ (NIH, USA); GraphPad Prism 8.4.2, USA
Vortex	VWR, USA

Table 3.7: General Equipment used in this study (cont.)

Equipment	**Supplier**
Water Purification	WA-TECH UP Water Purification System, Germany
Waterbath	Memmert Water Bath, Germany

4. METHODS

4.1. Cell Culture

HK-2 and WB-F344 cells were cultured in DMEM/F12 supplemented with 10% Fatal Bovine Serum, 1% (v/v) Penicillin (100U/mL)-Streptomycin (100µg/mL), and 1% (v/v) L-Glutamine at 37oC (Complete Medium), 5% CO2 and humidified atmosphere. MEF cells were cultured in DMEM/F12 supplemented with 10% Fatal Bovine Serum, 1% (v/v) Penicillin (100U/mL)-Streptomycin (100µg/mL), 1% (v/v) L-Glutamine, and 1X MEM Non-Essential Amino Acids Solution at 37°C, 5% CO2 and humidified atmosphere. Cells were grown in 60 mm 100 mm or 150 mm cell culture dishes and were sub-cultured every other day. During chemical treatments, FBS amount was decreased to 5% (Assay Medium).

4.2. Chemicals and Treatments

Cells were treated with OTA for determined periods of time specific to the experimental set-up. Pre-determined doses of eIF2α kinase inhibitors C16, A92 and GSK'414 were treated to cells individually, approximately 2h before respective OTA treatment. 100 µM puromycin was treated to cells 15 minutes before sample collection, while 100 µM cycloheximide was treated separately as negative control, 30 min before puromycin. Cells were treated with 1 µM wortmannin and 50 nM rapamycin 1hprior to respective OTA treatments. Stock solutions of both were prepared with DMSO.

Stock solutions of OTA and cycloheximide were prepared in EtOH and control cells were treated with vehicle, 0.1% v/v EtOH. Stock solutions of C16, A92 and GSK2606414 (GSK'414) were prepared in DMSO, while the stock solution of puromycin was prepared in ddH2O. Stock solutions of C16, A92 and GSK'414 were stored at -80°C, while aliquots in use stored at -20°C. All of the stock solutions were stored at -20°C.

4.3. CVDK-8 Viability Assay

NutriCulture Cell Viability Detection Kit-8 (CVDK8) was used to determine viability of cells under experimental manipulations in HK-2, WB-F344 and MEF cells. Cells were seeded on 96-well plate at 1x104 cell/well density for HK-2 and MEF and 2x104 cell/well density for WB-F344 cells. After inhibitor and/or OTA treatments, at the time of sample collection, 10μl/well working solution of CVDK8 kit added on the cells. After 2h of incubation, absorbance values were measured at 450 nm wavelength by microplate reader.

4.4. Protein Extraction and Western Blotting

After each treatment, cells were rinsed with cold PBS and were lysed in RIPA supplied with protease and phosphatase inhibitors. RIPA was added to the cells on plate and cells were incubated on ice for at least 30 minutes or stored in -20 oC for a few days. If the cells were in -20 oC, they were thawed on ice. Then the cells were scraped. The lysates were incubated on ice for at least 30 minutes. Lysates were centrifuged at 14000 RPM at 4 °C for 15 min. Supernatant was collected as total protein lysate after centrifugation. Concentrations of the protein lysates were quantfied by Pierce™ BCA Protein Assay Kit according to its manual.

10-40 μg total protein lysates were mixed with 4X protein loading dye and denatured at 95 °C for 5 min, then loaded on the gel 10% resolving, 4% stacking SDS-Polyacrylamide gel. On stacking and resolving gel, proteins were run at 80V and 100V, respectively. After running, proteins were transferred to PVDF membrane using Bio-Rad SDS-PAGE transfer system. Membranes were blocked in blocking solution for at least for 45 min at RT. After blocking, membranes were washed with TBS-T 3 times for 5 min. Then membranes were incubated with primary antibody solution overnight at 4 °C. After first antibody incubation, membranes were washed with TBS-T 3 times for 5 min and incubated in HRP-linked second antibody (Rabbit or Mouse IgG) solution for at least 1h at RT. After second antibody incubation membranes were washed

again 3 times with TBS-T and incubated inhRP substrate-enhancer solution Clarity Western ECL Substrate for about 30 seconds. The protein bands were visualized with chemiluminescence visualization system Syngene and were analyzed by ImageJ image analysis software. GAPDH or β-actin was used as loading control.

4.5. SUnSET Method

To visualize global translation rates, the SUnSET (Surface Sensing of Translation) method was used. This technique relies on the incorporation of the antibiotic puromycin into nascent growing peptides on actively translating ribosomes, which can then be detected via Western blot using an anti-puromycin antibody (Aviner, 2020). For this purpose, 100μM puromycin was added to the cells 15 minutes before sample collection. As a negative control, 100μM cycloheximide was added to separate wells 30 minutes prior to puromycin treatment to inhibit translation. After treatment, cells were lysed and processed for Western blotting as described above. For statistical analysis, CHX-treated samples were excluded, as their near-complete inhibition of translation markedly skews variance and significance testing within experimental groups.

4.6. Statistical Analysis

Statistical analysis was performed with GraphPad Prism 8.4.2 software. The data were shown as mean $\pm$ standard error of the mean, and for comparisons, ANOVA and Bonferroni (as post-hoc) were used. The data were first normalized to the loading control (GAPDH or β-actin) and then to the control sample to calculate the fold-change, as presented in the figures. The number of independent replicas is represented as "n" on each graph in the figures. Significance vs. control: ns: non-significant, $^{*}p < 0.05$, $^{**}p < 0.01$, $^{***}p < 0.001$, $^{****}p < 0.0001$. Significance between non-control groups: $\#p < 0.05$, $\#\#p < 0.01$, $\#\#\#p < 0.001$, $\#\#\#\#p < 0.0001$.

5. RESULTS

5.1. Investigation of the Time-Dependent Effects of OTA on eIF2α Phosphorylation and Global Translation Rate

Eukaryotic initiation factor (eIF2) complex is responsible for the recruitment of the initiator methionyl-transfer RNA to translation initiation complex on mRNAs while phosphorylation of α subunit on eIF2 results in inhibition of such recruitment and leads to subsequent decreased in 5'cap dependent (i.e. global) translation rate (Krishnamoorthy *et al.*, 2001). In the literature, it was shown that dose-dependent OTA exposure increases eIF2α phosphorylation in human proximal tubular epithelial (HK-2) cell line (Deng *et al.*, 2023); however, there is no time-dependent experiment and there is no study available to show the link in OTA-induced eIF2α phosphorylation and inhibition of protein synthesis simultaneously.

As part of this thesis, the mechanism of eIF2α phosphorylation and subsequent inhibition of global translation rate is investigated across different cell lines. For this purpose, HK-2 and rat liver progenitor (WB-F344) cells were treated with vehicle for 24h (Ctr) or 10 μM OTA for 1, 3, 6, 12, 24h, then eIF2α and p-eIF2α levels were visualized with Western Blot Analysis. Global translation rate for the same set-ups were observed with surface sensing of translation (SUnSET) method, in which 100 μM puromycin (PURO) treated to cells before sample collection while cycloheximide (CHX) treated as a negative control. OTA increased p-eIF2α levels significantly at 12 and 24h while decreasing global translation rate significantly at 6, 12 and 24h in HK-2 cells (Figure 5.1). On the other hand, for WB-F344 cells, p-eIF2α increase were significant at 6 and 12h time-points and decreased significantly at 24h, the same manner of action observed also in the global translation inhibition rate (Figure 5.2).

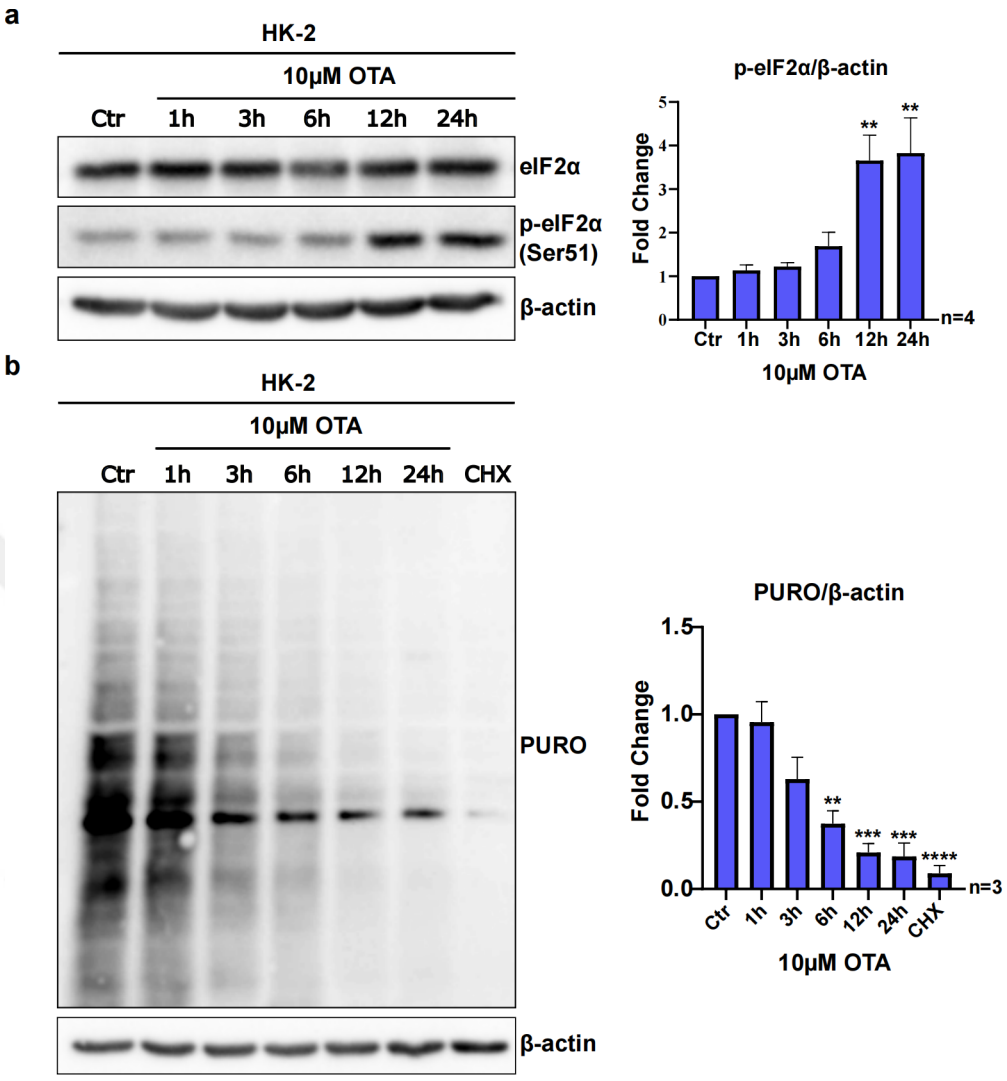

Figure 5.1: Time-dependent effects of OTA on p-eIF2α and global translation in HK-2 cells. OTA induces (a) p-eIF2α and (b) global translation inhibition in a time-dependent manner. HK-2 cells were treated with vehicle (Ctr) or 10 μM OTA for the indicated times. Data are shown as fold change vs. vehicle (mean $\pm$ SEM; n = independent replicates).

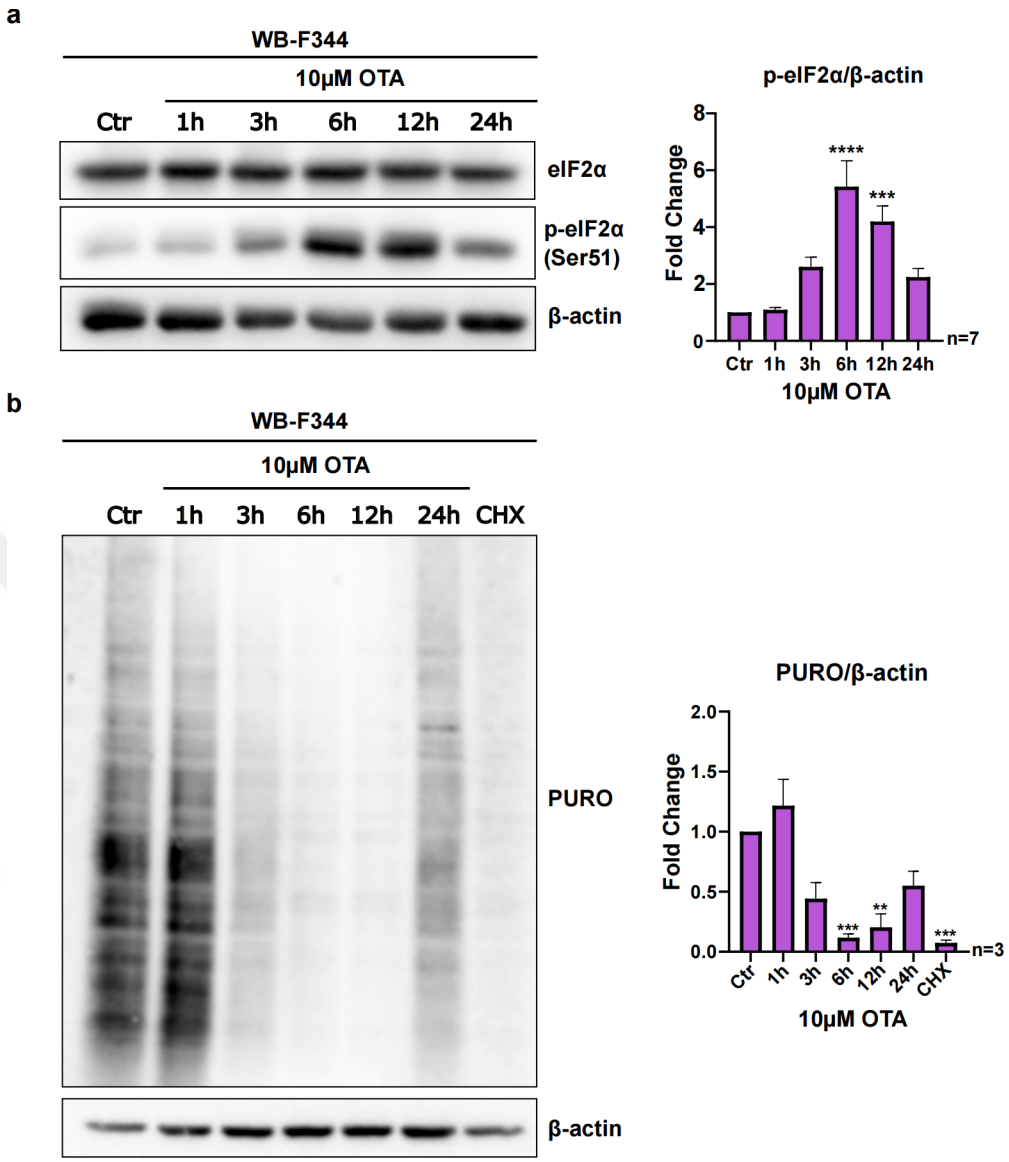

Figure 5.2: The time-dependent effects of OTA on p-eIF2α and global translation in WB-F344 cells. OTA induces (a) p-eIF2α and (b) global translation inhibition in time-dependent manner in WB-F344 cells, visualized with Western Blot analysis. The cells were treated with vehicle in Ctr or 10 μM OTA for indicated time periods.

In the literature, a dose of 10 μM was identified as subtoxic for MEF cells (Akpinar *et al.*, 2019). However, our cells exhibited heightened sensitivity to OTA exposure at this concentration. This discrepancy may be attributed to cellular sensitization following mycoplasma clearance via antibiotic treatment. Certain antibiotics, that are

also used for mycoplasma treatments, have been reported to modulate stress response pathways and alter drug sensitivity of eukaryotic and mammalian cells, which supports our notion (Kalghatgi *et al.*, 2013; Moullan *et al.*, 2015). Therefore, MEF cells were exposed to 24h OTA in dose-dependent manner as indicated in Figure 5.3a and the cell viability measured to determine the subtoxic dose in which most cells live, while OTA toxicity is still visible. In 7.5 μM treatment approximately 86.3% cells were viable while the viability decreased to 51.8% and 21.6% in 10 μM and 15 μM OTA exposure respectively (Figure 5.3a). Subsequently, p-eIF2α and global translation levels of time-dependent 7.5 μM OTA treatment in MEF cells were visualized. Result indicated peak increase in p-eIF2α (Figure 5.3b) and likewise decrease in global translation at 6h time-point (Figure 5.3c).

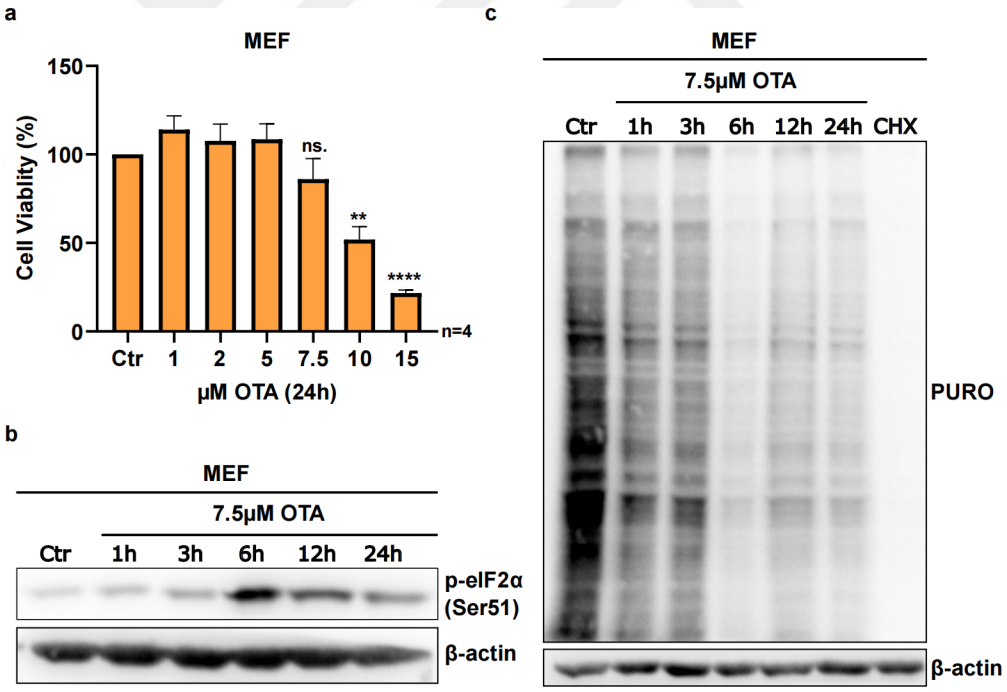

Figure 5.3: The cell vialibity under dose-dependent OTA exposure, and time-dependent effects of OTA on p-eIF2α and global translation in MEF cells. (a) Cell viability of OTA exposure at indicated concentrations for 24h. OTA induces (b) p-eIF2α and (c) global translation inhibition in time-dependent manner in MEF cells, visualized with Western Blot analysis.

5.2. Investigation of the Effects of eIF2α Kinase Inhibition on OTA-Induced Toxicity

The phosphorylation of eIF2α can be induced by four different kinases namely PKR, GCN2, PERK and HRI, depending on the environmental stress conditions (Pakos-Zebrucka *et al.*, 2016). Even though PERK has been indirectly suggested as a potential kinase responsible for OTA-induced eIF2α phosphorylation (Deng *et al.*, 2023), there is no evidence on the involvement of other kinases or experimental proof confirming this mechanism.

Since ER stress, oxidative stress, and amino acid starvation, known to activate PKR, PERK, and GCN2, respectively, have already been associated with OTA-induced toxicity (Deng *et al.*, 2023; Wang *et al.*, 2022; Yang *et al.*, 2023), these kinases stand out as strong candidates responsible for OTA-induced eIF2α phosphorylation. Exploiting the extensively studied and commercially accessible specific chemical inhibitors, namely C16, GSK2606414 (GSK'414), and A92, which selectively target PKR, PERK, and GCN2, respectively (Bagratuni *et al.*, 2020; Brazeau and Rosse, 2014; Jammi *et al.*, 2003), their involvement was investigated to elucidate the underlying mechanism of OTA toxicity.

5.2.1. Dose- Dependent Effects of eIF2α Kinase Inhibitors on eIF2α Phosphorylation and Global Translation Under OTA exposure

The eIF2α kinases play a central role in integrated stress response (ISR) mechanisms and manipulation of one might result in cross-activation of a sister kinase. Therefore, taking into the valuable study of Szaruga and colleagues on the inhibitors of interest (Szaruga *et al.*, 2023), dose-dependent experiments were conducted to identify the inhibitory doses that cause no cross-interaction of another kinase while interfering with OTA-induced toxicity. For this purpose, 0.25, 0.5, 1, 5, 10 μM for C16 and GSK'414; while 0.5, 1, 2.5, 5, 10 μM concentrations for A92 chosen. HK-2 and WB-F344 cells were treated with above mentioned dosages of inhibitors in the presence

or absence of 10 μM OTA for 12h. In HK-2, at 1 μM C16 (Figure 5.4a) and 1 μM A92 (Figure 5.4b) treatments, p-eIF2α levels remained similar to the control even in the presence of OTA, despite OTA alone induced a marked increase in p-eIF2α levels. Higher concentrations of only C16 or A92 treatments showed increased p-eIF2α compared to control samples, indicating possible unwanted cross-activity of a sister kinase. On the other hand, GSK'414 treatment did not substantially reduce OTA-induced p-eIF2α levels (Figure 5.4c); therefore, 1 μM was chosen as the selected concentration, as it is an effective dose reported in the literature (Szaruga *et al.*, 2023) that also does not appear to cross-activate other kinases in this experiment.

Similarly in WB-F344 cells, 1 μM C16 and 5 μM A92 were the effective dosages that decreased OTA-induced p-eIF2α, whereas GSK'414 did not demonstrate such an effect and was also selected as 1 μM for consistency (Figure 5.5).

In MEF cells, same concentrations of inhibitors treated with or without 7.5 μM OTA for 6h, and effective dosages were 1 μM C16 and 2.5 μM A92 while GSK'414 did not have substantial effect on p-eIF2α phosphorylation, so 1 μM used for further experiments (Figure 5.6).

These findings demonstrate selective modulation of ISR pathways at the selected inhibitor concentrations, effectively minimizing cross-kinase activation and facilitating the identification of optimal dosages to dissect kinase-specific contributions to OTA-induced stress signaling.

Building upon these data, the selected doses (Table 5.1) were repeated with or without OTA co-treatment to examine p-eIF2α levels along with changes in global translation via SUnSET method, visualized as Western Blot image and statistical analysis conducted.

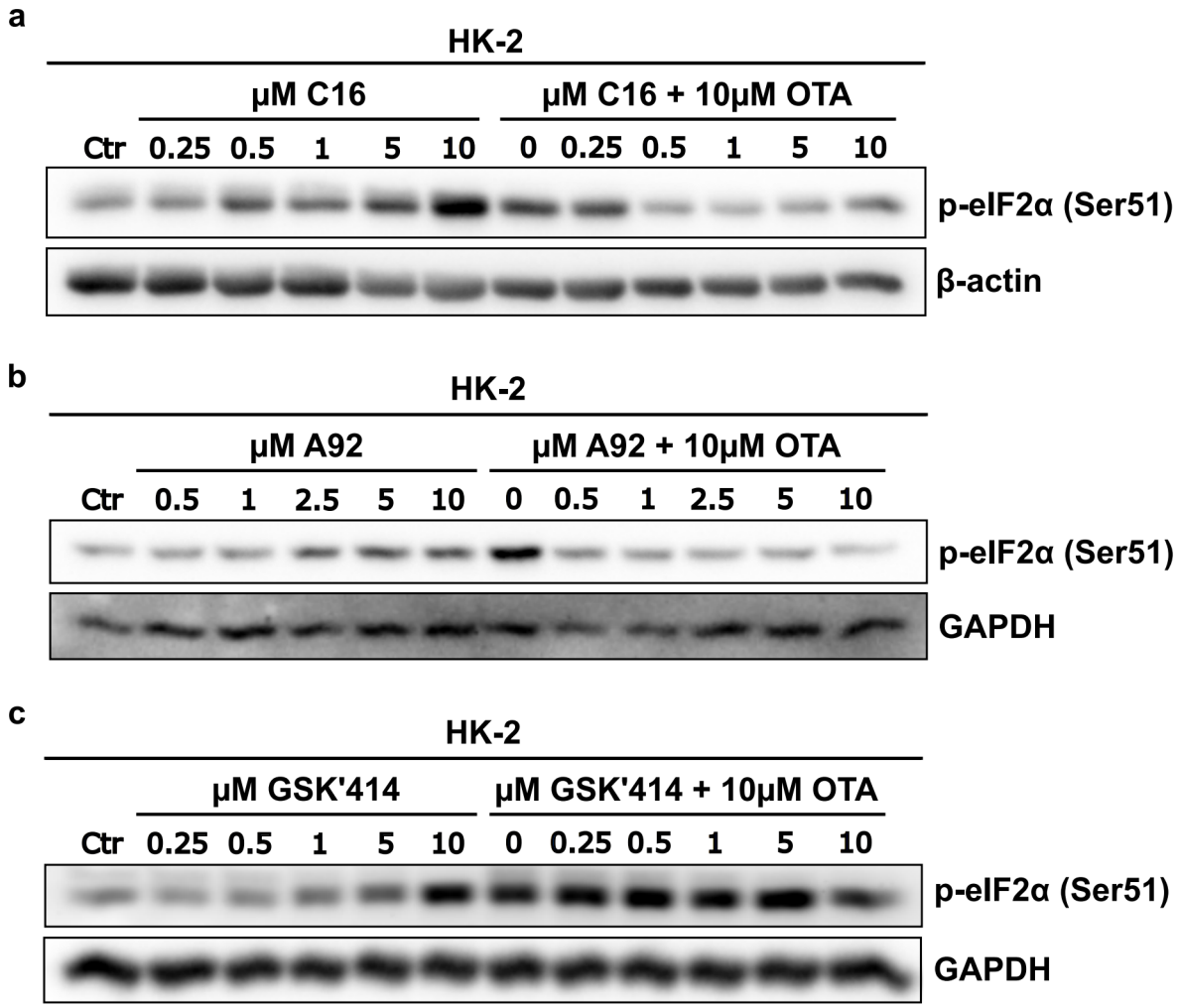

Figure 5.4: Dose-dependent assessment of ISR kinase inhibitors on p-eIF2α levels under 12h OTA expoure in HK-2. Cells were treated with increasing concentrations of the ISR kinase inhibitors (a) C16 (0.25-10 μM), (b) A92 (0.5-10 μM), and (c) GSK'414 (0.25-10 μM) in the presence or absence of 10 μM OTA for 12h. GAPDH or β-actin was used as a loading control.

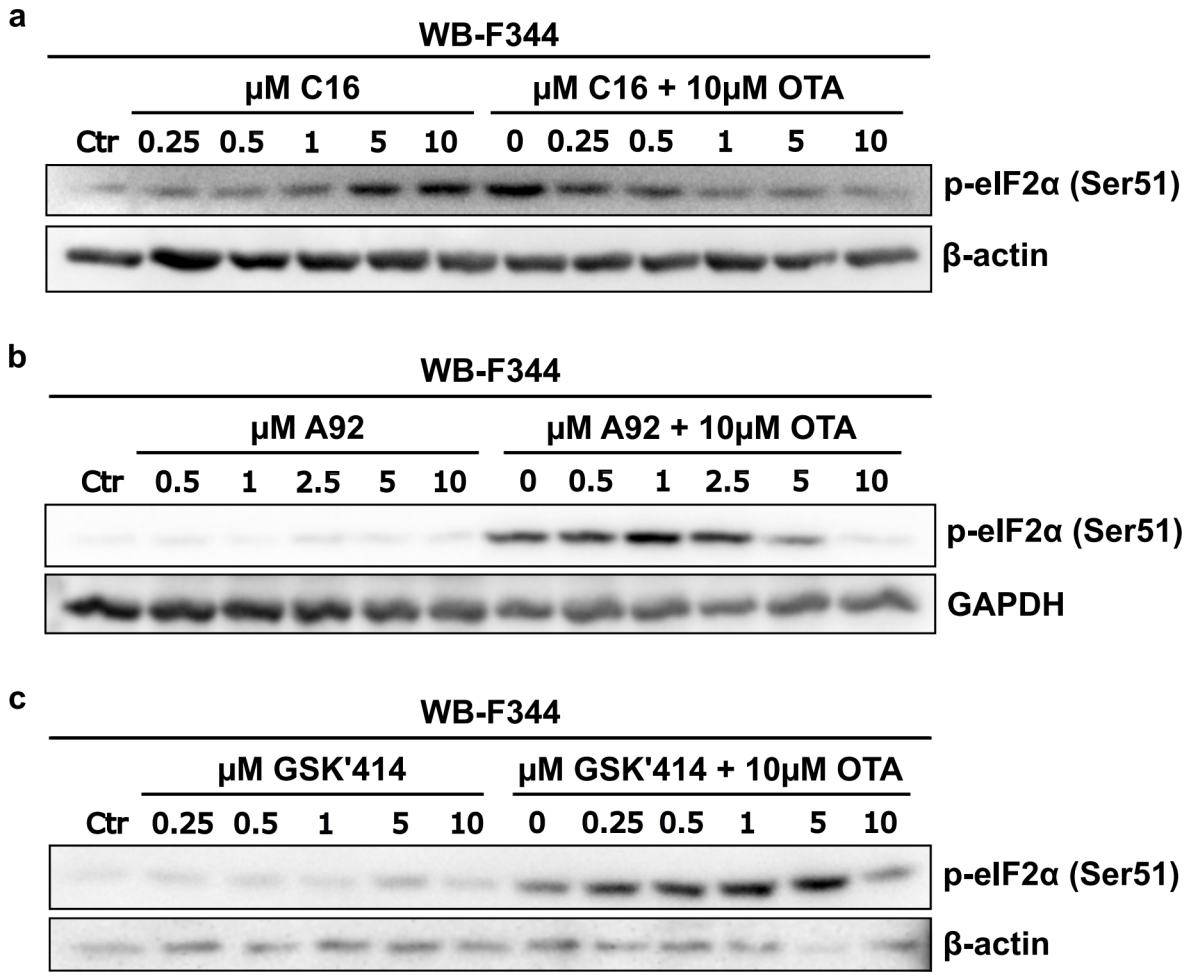

Figure 5.5: Dose-dependent assessment of ISR kinase inhibitors on p-eIF2α levels in response to 12h OTA treatment in WB-F344. Cells were treated with increasing concentrations of the ISR kinase inhibitors (a) C16 (0.25-10 μM), (b) A92 (0.5-10 μM), and (c) GSK'414 (0.25-10 μM) in the presence or absence of 10 μM OTA for 12h. GAPDH or β-actin was used as a loading control.

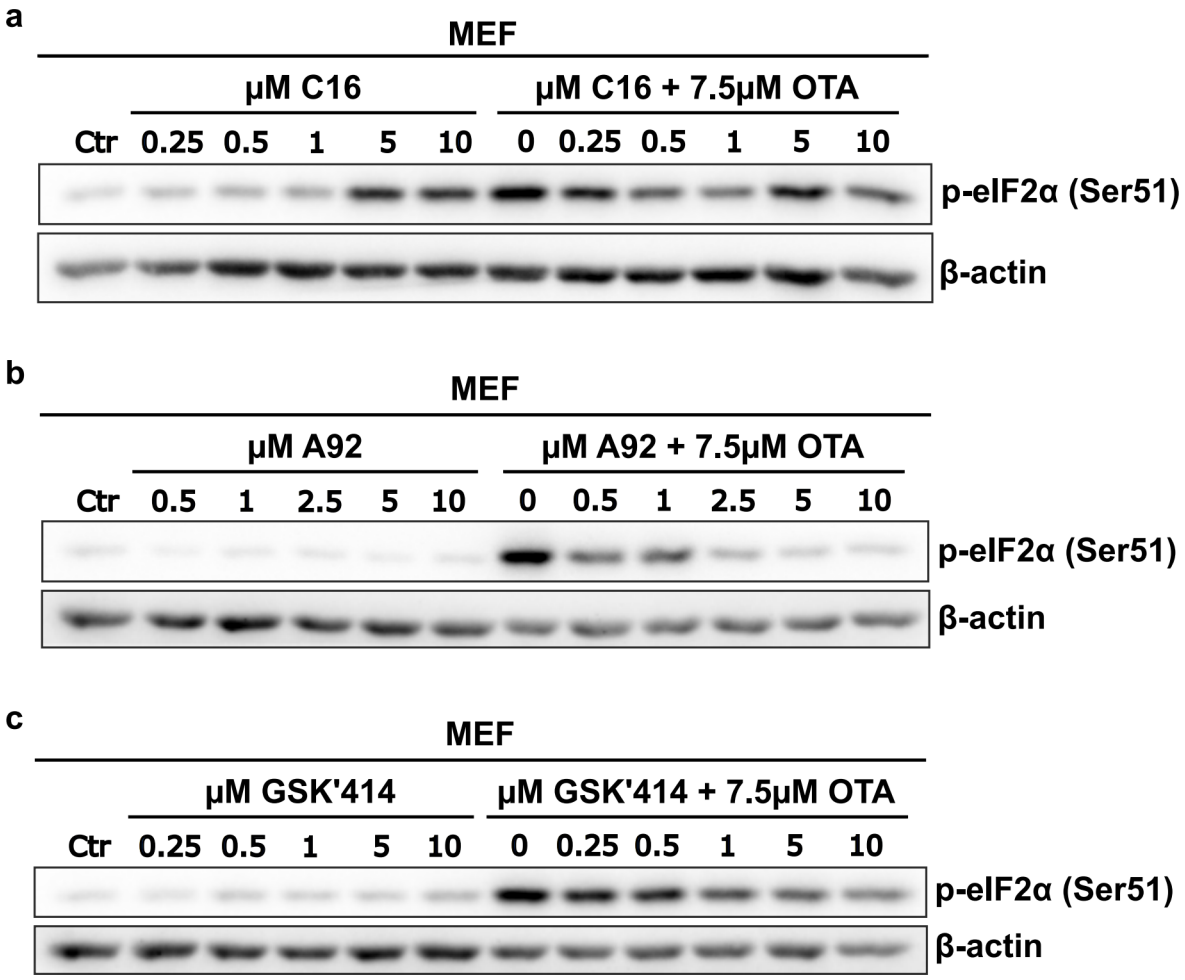

Figure 5.6: Dose-dependent assessment of ISR kinase inhibitors on p-eIF2α levels in response to 6h OTA treatment in MEF. Cells were treated with increasing concentrations of the ISR kinase inhibitors (a) C16 (0.25-10 μM), (b) A92 (0.5-10 μM), and (c) GSK'414 (0.25-10 μM) in the presence or absence of 7.5 μM OTA for 6h. β-actin was used as a loading control.

Table 5.1: Doses chosen for PKR, GCN2 and PERK inhibitors on different cell lines.

Cell Line	Inhibitor Doses		
HK-2	1μM C16	1μM A92	1μM GSK'414
WB-F344	1μM C16	5μM A92	1μM GSK'414
MEF	1μM C16	2.5μM A92	1μM GSK'414

To investigate the impact of ISR kinase inhibition on OTA-induced eIF2α phosphorylation and translational repression, HK-2 cells were treated with the selected inhibitor concentrations (1 μM C16, 1 μM A92, 1 μM GSK'414), with or without OTA co-treatment for 12h. Western blot analysis revealed that OTA treatment alone induced a marked increase in p-eIF2α levels, consistent with activation of the integrated stress response. Co-treatment with C16 or A92 significantly reduced OTA-induced p-eIF2α levels, while GSK'414 caused only a modest decrease (Figure 5.7a). However, the global translation levels, assessed by the SUnSET method, showed a divergent pattern. Despite the reduction in p-eIF2α, co-treatment with C16 did not restore translation levels suppressed by OTA. In contrast, A92 and GSK'414 co-treatments partially recovered global translation compared to OTA alone (Figure 5.7b). These findings suggest that GCN2 and PERK inhibition may alleviate OTA-induced translational repression to a limited extent, whereas PKR inhibition reduces p-eIF2α without improving translation, indicating that reduction in p-eIF2α alone is not sufficient to restore translation under OTA-induced stress.

Similar experimental set-ups were applied to WB-F344 cells to assess cell-type specific effects further. Consistent with HK-2 data, OTA treatment led to a clear increase in p-eIF2α and a marked reduction in global translation. Co-treatment with C16 or A92 effectively reduced OTA-induced p-eIF2α levels, with A92 showing a more pronounced effect (Figure 5.8a). In contrast to HK-2 cells, both C16 and A92 also partially restored global translation in WB-F344 cells (Figure 5.8b), indicating that suppression of eIF2α phosphorylation by PKR or GCN2 inhibition was sufficient to relieve translational repression in this context. Notably, GSK'414 (PERK inhibitor) did not reduce p-eIF2α levels and appeared to further enhance OTA-induced phosphorylation, suggesting possible compensatory activation of other eIF2α kinases. Correspondingly, GSK'414 co-treatment failed to improve translation, suggesting a limited role for PERK in OTA-induced stress signaling in WB-F344 cells.

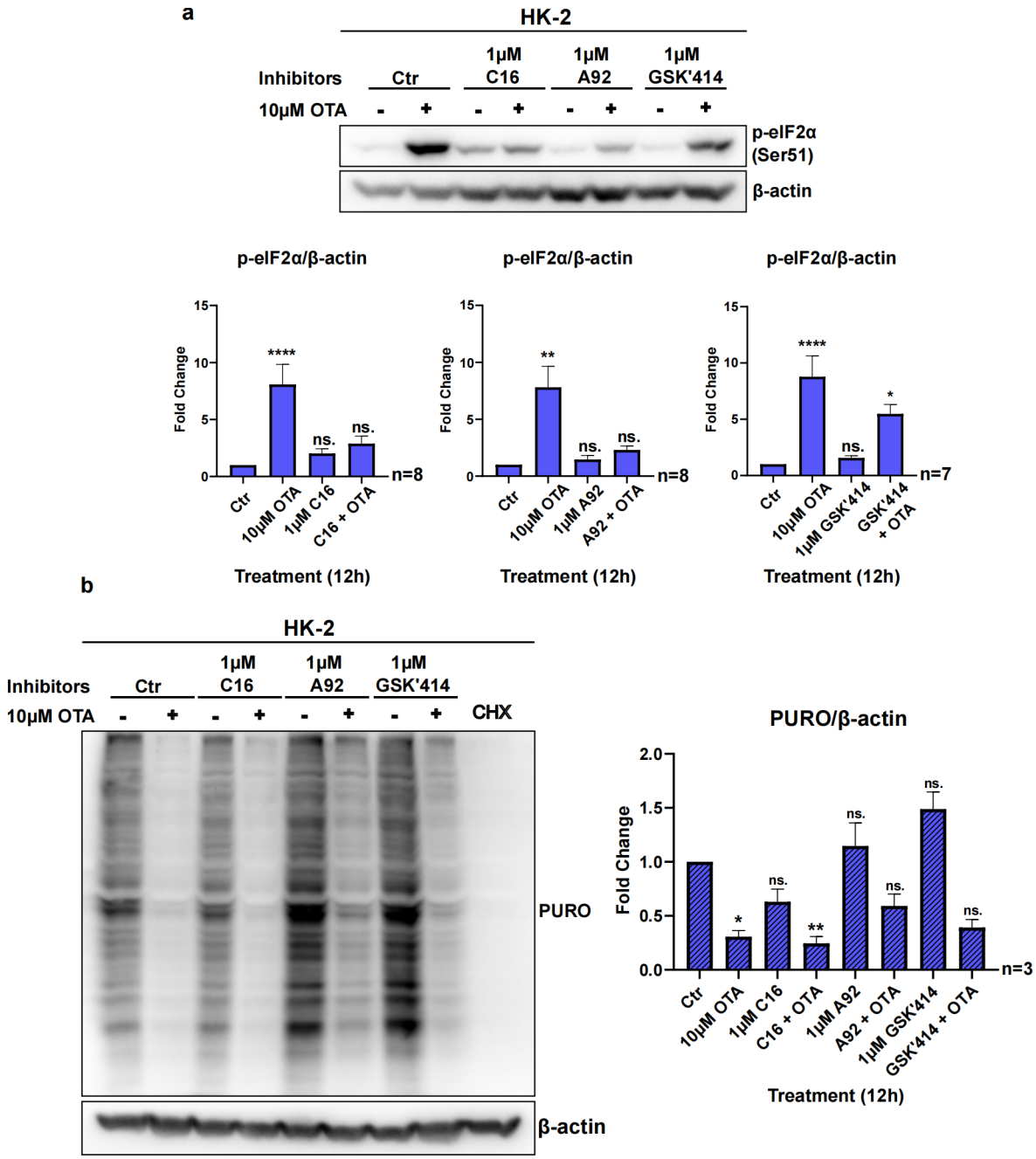

Figure 5.7: Effect of eIF2α kinase inhibition on OTA-induced eIF2α phosphorylation and global translation in HK-2 cells. HK-2 cells were treated with 10μM OTA, eIF2α kinase inhibitors (1μM C16, A92, or GSK'414), or combinations for 12h. Western blots show (a) p-eIF2α, and (b) puromycin incorporation (SUnSET assay).

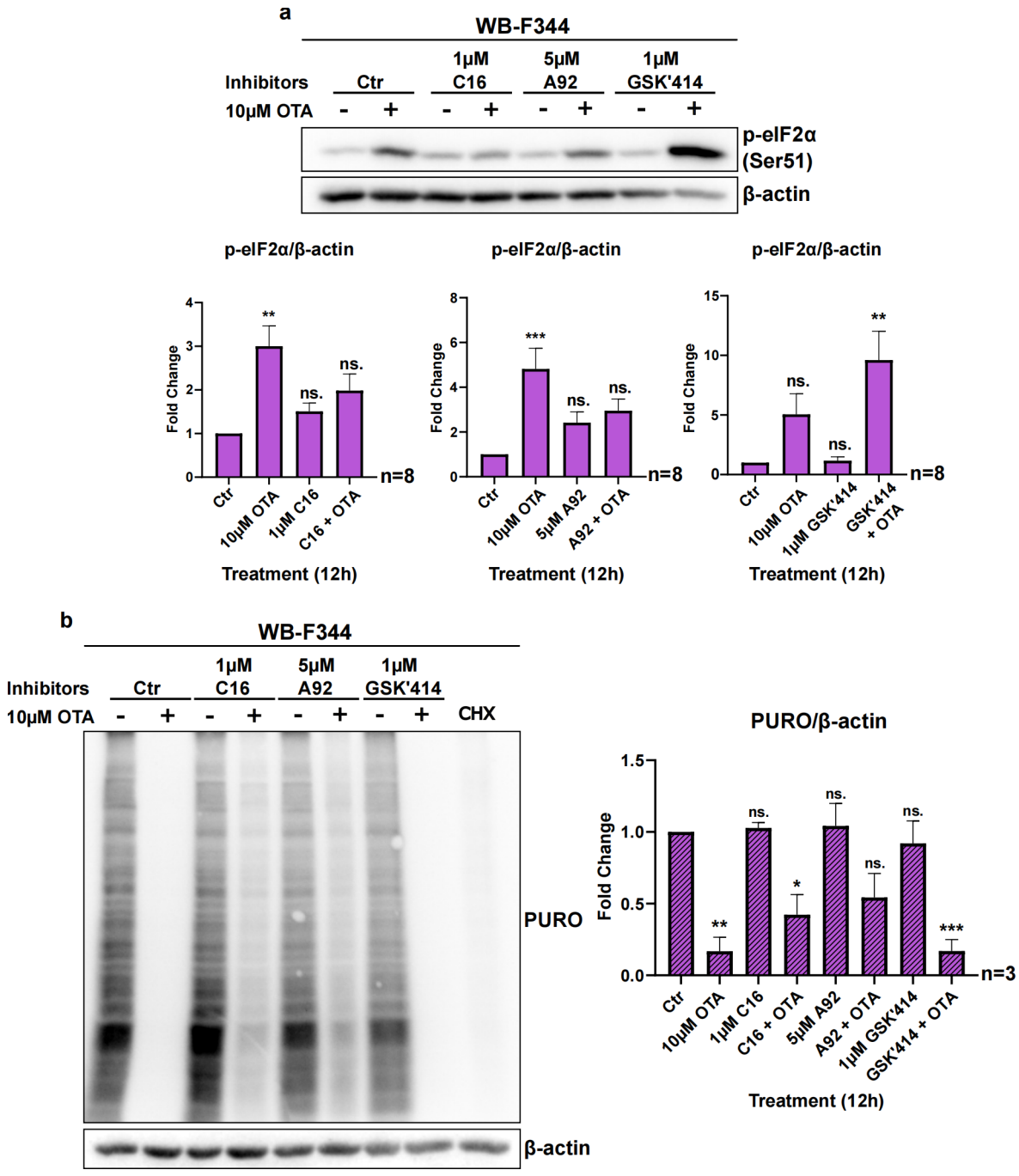

Figure 5.8: Effect of eIF2α kinase inhibition on OTA-induced eIF2α phosphorylation and global translation WB-F344 cells. HK-2 cells were treated with 10μM OTA, eIF2α kinase inhibitors (1μM C16, 5μM A92, or 1μM GSK'414), or combinations for 12h. Western blots show (a) p-eIF2α, and (b) puromycin incorporation (SUnSET assay).

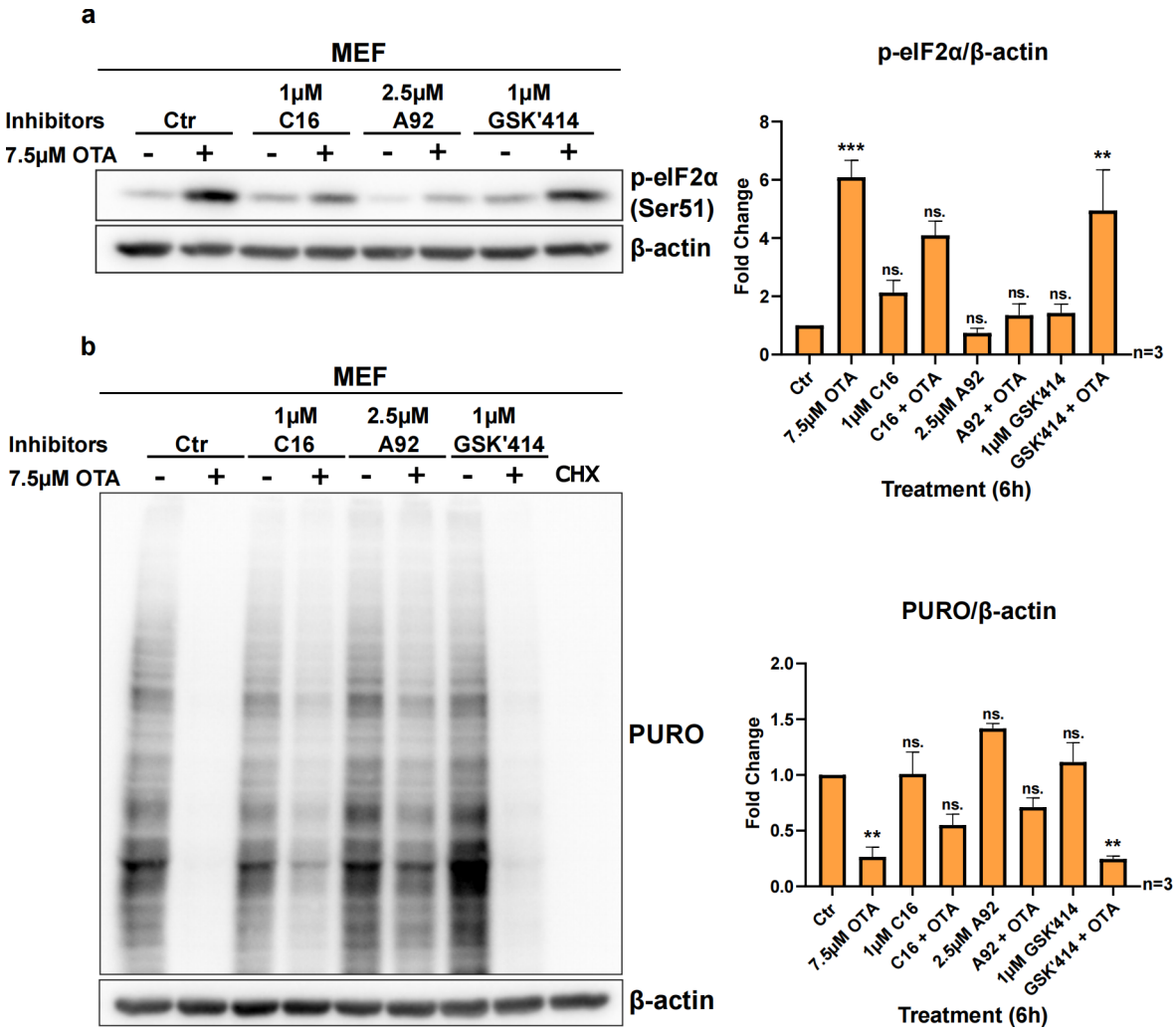

Figure 5.9: Effect of eIF2α kinase inhibition on OTA-induced eIF2α phosphorylation and global translation MEF cells. MEF cells were treated with 7.5μM OTA, eIF2α kinase inhibitors (1μM C16, 2.5μM A92, or 1μM GSK'414), or combinations for 6h. Western blots show (a) p-eIF2α, and (b) puromycin incorporation (SUnSET assay).

The same experimental design was applied to MEF cells using the selected inhibitor concentrations, with analysis performed after 6h of OTA exposure, based on peak p-eIF2α timing established previously. As in HK-2 and WB-F344 cells, OTA treatment led to a clear increase in p-eIF2α levels and a strong reduction in global translation (Figure 5.9). Co-treatment with A92 (GCN2 inhibitor) markedly reduced OTA-induced p-eIF2α levels and partially restored translation. C16 (PKR inhibitor) also lowered p-eIF2α and led to a moderate recovery in translation, although less pro-

nounced than A92. In contrast, GSK'414 (PERK inhibitor) did not reduce p-eIF2α levels and had minimal impact on OTA-induced translation repression. These findings indicate that in MEF cells, inhibition of GCN2 and, to a lesser extent, PKR, can mitigate OTA-induced translational repression, while PERK inhibition remains ineffective, consistent with trends observed in HK-2 and WB-F344 cells.

5.2.2. Effects of eIF2α Kinase Inhibitions on OTA-induced Cell Death

Based on the literature and our previous experiments, we have determined optimal effective doses where in vitro OTA toxicity is most pronounced. Approximately 20% of cells undergo cell death, and cellular responses such as deregulation of signaling pathways are observed following 24h treatment with OTA at utilized doses; nevertheless, the majority of cells (80%) remain viable (Akpinar *et al.*, 2019; Ozcan *et al.*, 2015). Since inhibition of eIF2α kinases led to a partial increase in global translation rates in a cell type–specific manner at time points showing peak eIF2α phosphorylation, we examined their effects on OTA-induced cell death both at those earlier time points and at 24h.

At 12h, treatment with 10μM OTA slightly reduced HK-2 cell viability compared to the untreated control cells, while 1μM C16 alone did not significantly alter viability. Co-treatment with C16 and OTA led to a further significant reduction in cell viability compared to control and was significantly lower than C16 alone, indicating that C16 did not rescue OTA-induced cytotoxicity. Similarly, both A92 and GSK'414 treatments reduced viability compared to control and their co-treatments with OTA led to further reductions, with significantly lower viability than A92 or GSK'414 alone (Figure 5.10a). At 24h, OTA-induced cytotoxicity was even more severe, with viability dropping further. All inhibitors alone (C16, A92, GSK'414) significantly decreased viability compared to control. Combination treatments with OTA resulted in the most substantial reductions in cell viability, with significant differences compared to inhibitor-only groups (Figure 5.10b). Notably, A92 + OTA and GSK'414 + OTA showed the lowest cell viability overall. These findings indicate that ISR inhibitors not only fail to pro-

tect against OTA-induced cytotoxicity but may exacerbate cell death when combined, especially after 24h of treatment.

In line with findings from HK-2, eIF2α kinase inhibition also altered OTA-induced cytotoxicity in WB-F344 liver progenitor cells, revealing cell type-specific differences in stress response dynamics. While OTA alone had little to no effect on viability at 12h and caused only moderate cytotoxicity at 24h, inhibition of GCN2 using A92 led to a pronounced reduction in cell viability at both time points, even in the absence of OTA, highlighting a critical survival role for GCN2 in this cell type. Similarly, co-treatment with GSK'414 and OTA significantly decreased viability at 24h, despite GSK'414 alone being non-toxic. In contrast, C16 had little impact at 12h but notably reduced viability at 24h, particularly in combination with OTA, suggesting that PKR contributes to longer-term survival under sustained OTA stress in WB-F344 cells (Figure 5.11).These findings support the idea that ISR kinase function and its contribution to OTA sensitivity is highly context-dependent, shaped by intrinsic stress adaptation mechanisms of each cell type.

Consistent with cell line–specific ISR modulation patterns, MEF cells exhibited a distinct cytotoxic profile upon OTA exposure and ISR kinase inhibition. At 6h, treatment with 7.5μM OTA alone or in combination with C16 or GSK'414 did not significantly affect cell viability, indicating limited acute cytotoxicity in this early phase. However, inhibition of GCN2 using A92 significantly reduced viability both alone and in combination with OTA where combinatorial condition displaying stronger toxicity compared to A92 alone (Figure 5.12a).

By 24h, OTA treatment alone led to a moderate but significant reduction in viability, with A92 again showing pronounced cytotoxic effects both alone and when combined with OTA. Interestingly, GSK'414 and OTA co-treatment caused a substantial reduction in viability, while GSK'414 alone remained non-toxic at given concentration.

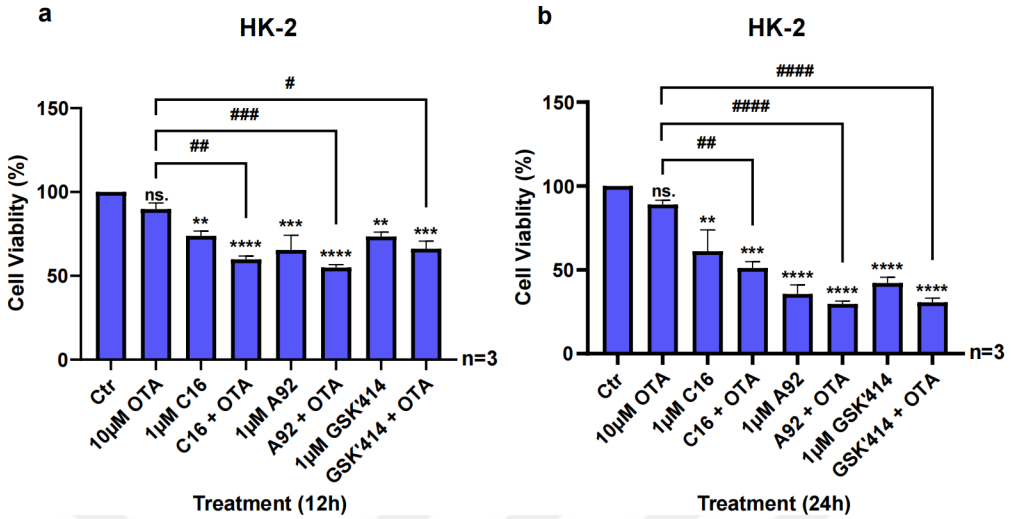

Figure 5.10: Effect of ISR kinase inhibition on OTA-induced cytotoxicity in HK-2 cells. HK-2 cells were treated with 10 μM OTA, PKR inhibitor C16 (1 μM), GCN2 inhibitor A92 (1 μM), or PERK inhibitor GSK'414 (1 μM), alone or with 10 μM OTA for (a) 12 h and (b) 24 h.

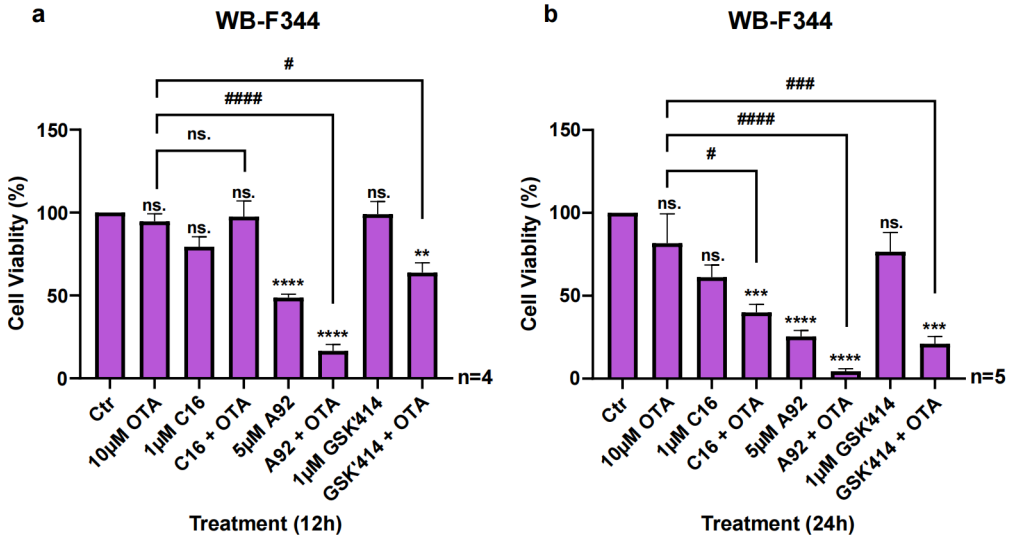

Figure 5.11: Effect of ISR kinase inhibition on OTA-induced cytotoxicity in WB-F344 cells. Cells were treated with 10 μM OTA, PKR inhibitor C16 (1 μM), GCN2 inhibitor A92 (5 μM), or PERK inhibitor GSK'414 (1 μM), alone or with 10 μM OTA for (a) 12 h and (b) 24 h.

C16, either alone or with OTA, did not dramatically alter viability at either time point (Figure 5.12b). These results demonstrate that MEFs, like the other cell lines, respond to ISR inhibition in a kinase- and time-dependent manner, with GCN2 and PERK inhibition showing the greatest impact on cell survival under OTA stress.

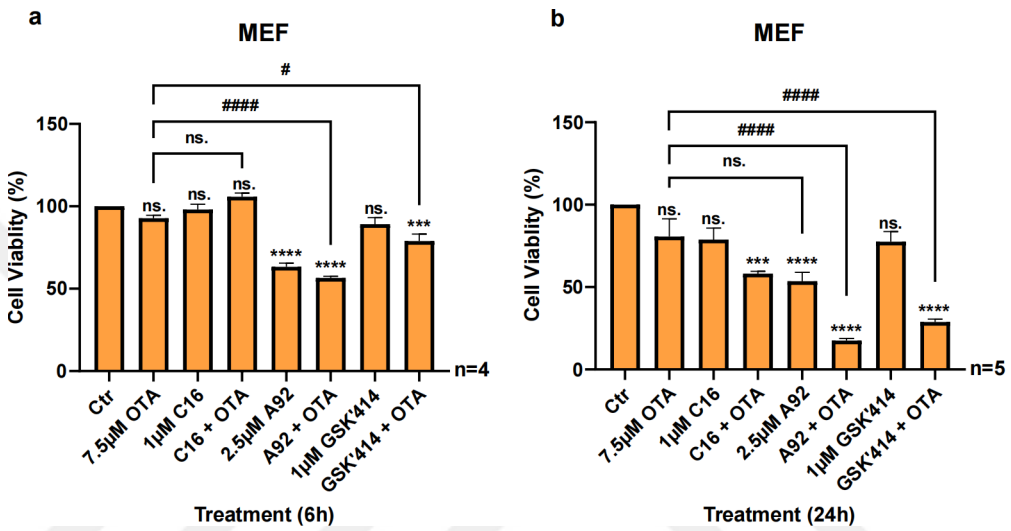

Figure 5.12: Effect of ISR kinase inhibition on OTA-induced cytotoxicity in MEF cells. Cells were treated with 7.5 μM OTA, PKR inhibitor C16 (1 μM), GCN2 inhibitor A92 (2.5 μM), or PERK inhibitor GSK'414 (1 μM), alone or with 7.5 μM OTA for (a) 6 h and (b) 24 h.

Across all three cell lines, OTA treatment resulted in a time-dependent reduction in cell viability, with the strongest effects observed at 24h. In all cell lines, co-treatment with the PERK inhibitor GSK'414 consistently reduced viability further than OTA alone at 24h, despite GSK'414 alone being non-toxic. A92 (GCN2 inhibitor) significantly decreased viability both alone and in combination with OTA in WB-F344 and MEF cells, while its effect was more moderate in HK-2 cells. In contrast, C16 (PKR inhibitor) had minimal impact on MEF viability, a delayed effect in WB-F344 cells, and moderate cytotoxicity in HK-2 cells when combined with OTA. These results indicate that while OTA-induced cytotoxicity and ISR kinase inhibition affect all three cell

lines, the magnitude and timing of responses differ depending on the kinase targeted and cell type.

5.3. Investigation of The Cross-Talk between PI3K/Akt/mTOR and eIF2α Phosphorylation under OTA exposure

OTA has been shown to activate PI3K/Akt/mTOR pathway, evidenced by increased phosphorylation of Akt as well as mTORC1 downstream targets p70 and pS6. Inhibition of PI3K/Akt activity by wortmannin has been reported to reduce cell viability, suggesting that OTA promotes cell survival through activation of this pathway (Ozcan *et al.*, 2015).

Phosphorylation of eIF2α has been associated with the PI3K/Akt/mTOR pathway in several studies, although the specific eIF2α kinase involved varies depending on the disease model or type of environmental stress of context (Jin *et al.*, 2021; Mounir *et al.*, 2011; Xu *et al.*, 2018). Even though OTA was reported to induce both Akt and eIF2α phosphorylation separately (Deng *et al.*, 2023; Ozcan *et al.*, 2015; Wang *et al.*, 2022), potential cross-talk between these survival pathways has not been previously explored.

5.3.1. Effects of eIF2α Kinase Inhibitions on PI3K/Akt/mTOR Pathway

While certain doses of eIF2α kinase inhibitors partially recovered protein synthesis inhibition under OTA exposure, the same doses exacerbated OTA-induced cell death dramatically. Since OTA exposure induces the PI3K/Akt/mTOR pathway to promote cell survival, the effect of eIF2α kinase inhibition on this pathway was also examined by checking key pathway components: p-Akt (Ser473), p-p70 (Thr389), and p-S6 (Ser235/236) at 12h of OTA exposure for HK-2 and WB-F344 cells, and 6h for MEF cells, corresponding to peak p-eIF2α induction. In all three cell lines, OTA treatment alone increased phosphorylation of Akt and its downstream targets, consistent with PI3K/Akt/mTOR pathway activation (Figure 5.13).

A92 treatments led to a marked decrease in p-Akt levels in all cell lines, while C16 showed substantial decrease in WB-F344 and MEF, and GSK'414 showed minimal decrease, even further increase in WBF-344 and MEF. On the other hand, the effect on downstream components showed more variations. In HK-2 cells, A92 and GSK'414 reduced p-p70 and p-S6 levels, while C16 had little effect. In WB-F344 and MEF cells, only A92 substantially decreased phosphorylation of p70 and S6, whereas C16 and GSK'414 did not significantly affect these targets (Figure 5.13). These results show that while both PKR and GCN2 inhibition suppress Akt activation under OTA stress, only GCN2 inhibition consistently reduces mTORC1 downstream signaling across all cell lines.

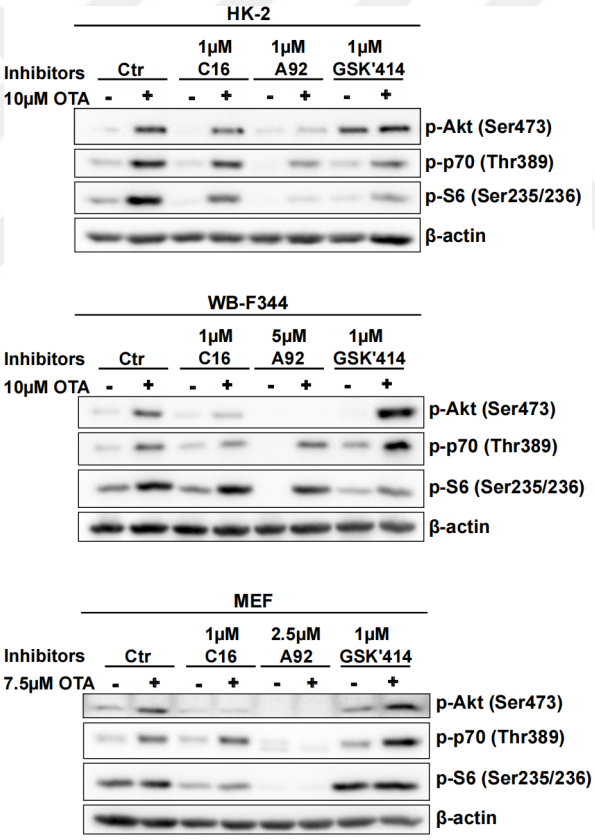

Figure 5.13: Effect of eIF2α kinase inhibition on PI3K/Akt/mTOR activation under OTA. HK-2 and WB-F344 cells were treated with 10 μM OTA for 12 h, and MEF with 7.5 μM for 6 h, with or without inhibitors (C16, A92, GSK'414). Western blotting for p-Akt, p-p70, and p-S6 assessed pathway activity, with β-actin as loading control.

5.3.2. Effects of PI3K/Akt and mTOR Inhibitions on eIF2α Phosphorylation

In order to further examine the cross-activation between these pathways, PI3K/Akt and mTORC activity was inhibited via wortmannin and rapamycin, respectively, and their effects on time-dependent OTA induced p-eIF2α levels investigated in HK-2 and WB-F344 cells. Inhibition efficiency was confirmed by reduced p-Akt levels following wortmannin treatment, and by reduced phosphorylation of p-p70 and p-S6 in response to rapamycin, confirming effective mTORC1 inhibition. In both cell lines, PI3K/Akt inhibition via wortmannin treatment resulted in a marked decrease in OTA-induced p-eIF2α levels, particularly at time points where p-eIF2α levels typically peaked following OTA treatment alone (Figure 5.14, Figure 5.15). This suggests that PI3K/Akt activity may support or sustain eIF2α phosphorylation under OTA-induced stress.

In contrast, mTORC1 inhibition showed a cell-type specific outcome. In WB-F344 cells, rapamycin had no detectable effect on OTA-induced p-eIF2α levels across time points, indicating that mTORC1 does not play a significant role in modulating ISR activation in these cells (Figure 5.15). In HK-2 cells, however, rapamycin treatment moderately reduced the fold increase in p-eIF2α levels compared to OTA alone (Figure 5.14). Despite this, HK-2 cells still exhibited significant p-eIF2α induction at the same peak time points as with OTA alone, suggesting that mTORC1 inhibition does not fully suppress OTA-induced ISR activation but may modulate its intensity.

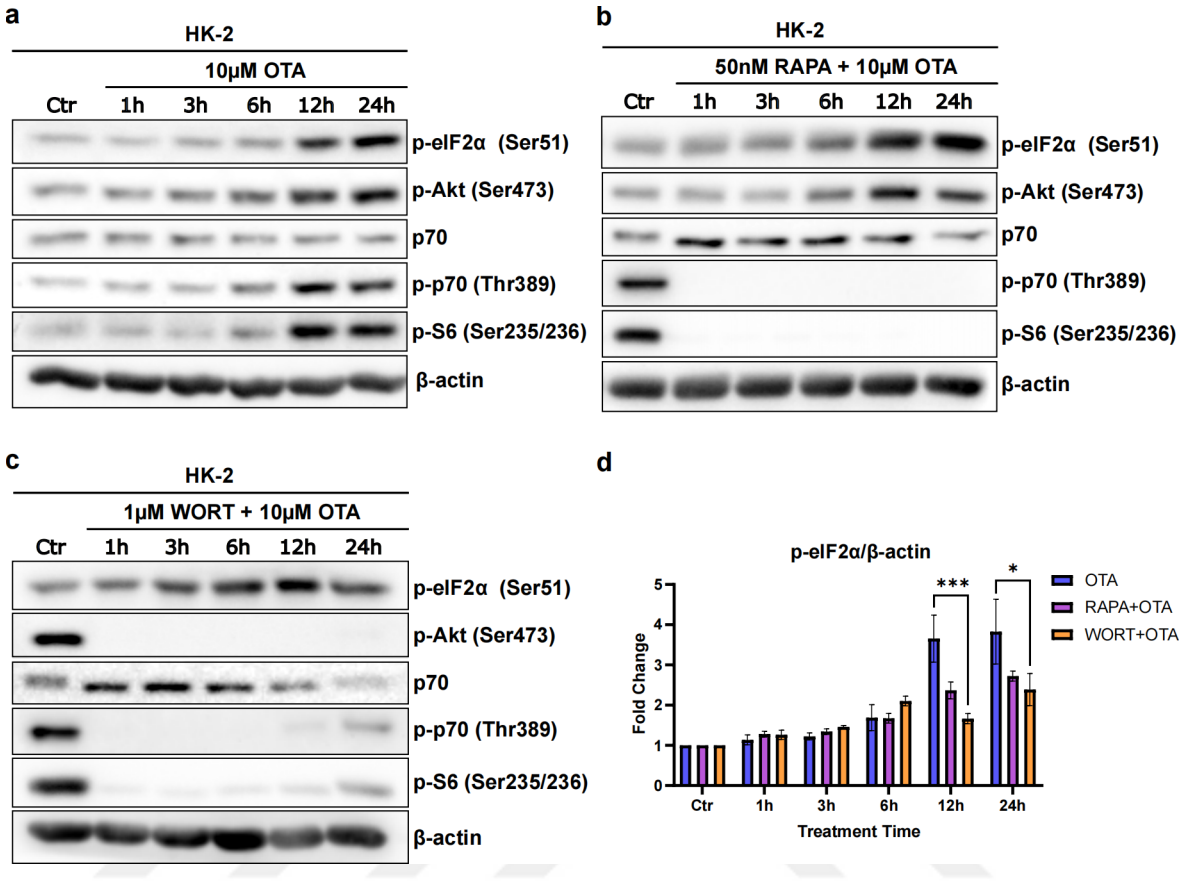

Figure 5.14: Effect of PI3K/Akt and mTORC1 inhibition on OTA-induced p-eIF2α in HK-2 cells. Cells were treated with 10 μM OTA ± wortmannin (1 μM) or rapamycin (50 nM). Western blots for p-eIF2α, p-Akt, p70, p-p70, and p-S6 confirmed effective inhibition; β-actin was loading control. Quantifications are fold change to control (mean ± SEM, n=4 for OTA; n=3 for WORT/RAPA)

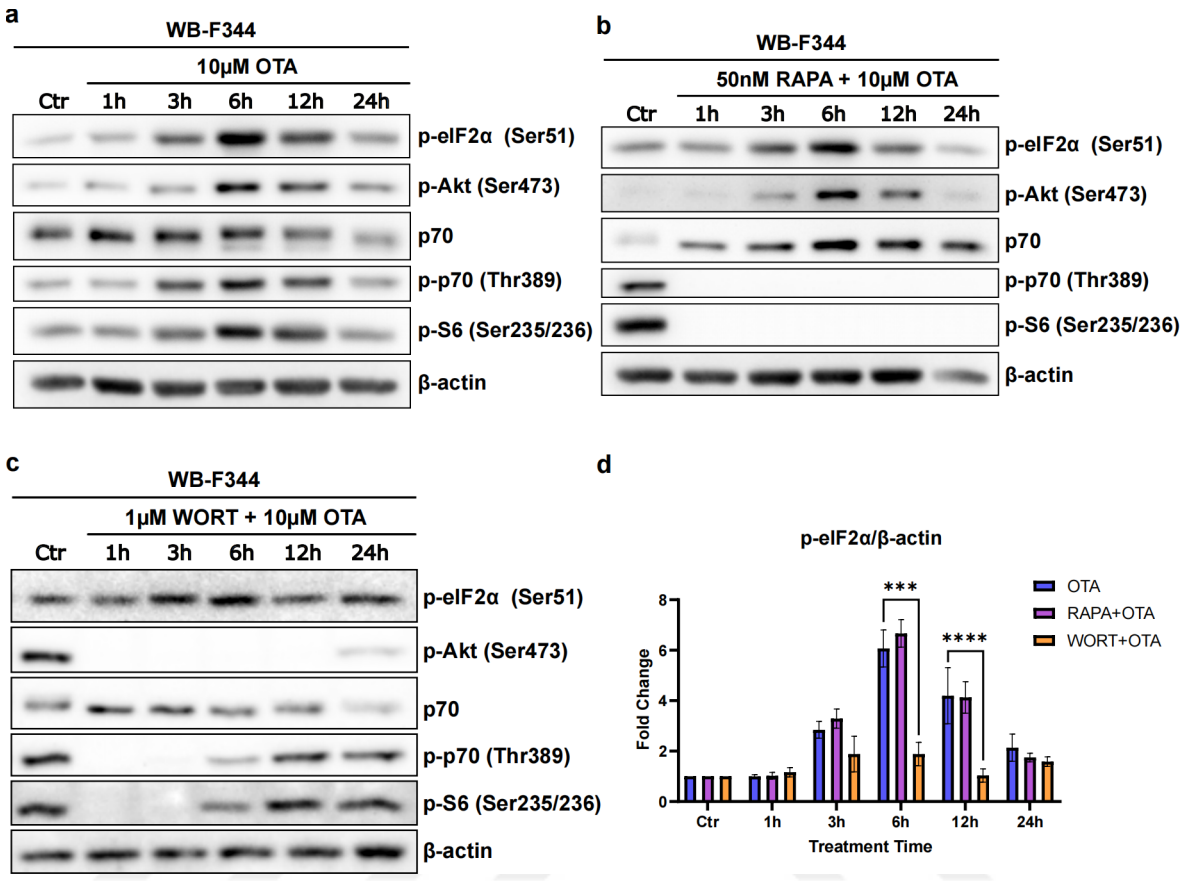

Figure 5.15: Effect of PI3K/Akt and mTORC1 inhibition on OTA-induced p-eIF2α in WB-F344 cells. Cells were treated with 10 μM OTA ± wortmannin (1 μM) or rapamycin (50 nM). Western blots for p-eIF2α, p-Akt, p70, p-p70, and p-S6 confirmed effective inhibition; β-actin was loading control. Quantifications are fold change to control (mean ± SEM, n=4 for OTA; n=3 for WORT/RAPA).

6. DISCUSSION

6.1. Mechanism of OTA-Induced eIF2α Phosphorylation and Global Translational Repression

In this thesis, the cellular responses to OTA-induced stress were investigated with a particular focus on global translational inhibition mechanisms governed by eIF2α phosphorylation and its interplay with survival pathways, namely PI3K/Akt/mTOR. OTA is a well-documented nephrotoxin known to disrupt cellular homeostasis through various stress signaling cascades, including oxidative stress, apoptosis, and survival pathways (Akpinar *et al.*, 2019; Ozcan *et al.*, 2015). One of the most consistently observed and mentioned effects of OTA in the literature is its capacity to inhibit protein synthesis, which is often linked to phosphorylation of eIF2α (Creppy *et al.*, 1983; Ozcan *et al.*, 2015). However, the identity of the eIF2α kinase(s) responsible for this phosphorylation event or the mechanism of the phenomenon under OTA exposure had remained unexplored, particularly across different cell types.

In accord with earlier reports demonstrating OTA disrupts protein synthesis by activating the Integrated Stress Response (ISR) (Creppy *et al.*, 1983; Deng *et al.*, 2023), time-course experiments confirmed a robust, time-dependent rise in p-eIF2α accompanied by a marked decline in global translation in HK-2, WB-F344, and MEF cells (Figure 5.1, Figure 5.2, Figure 5.3). Building upon the defined peak phosphorylation time-points, specific chemical inhibitors- C16, A92, and GSK'414-were used to inhibit PKR, GCN2, and PERK, respectively, in order to determine which kinase(s) contribute to phosphorylation for each cell-type. Dose-response analyses first established concentrations that decreased OTA-induced p-eIF2α without inducing cross-activation of sister kinases, enabling a clean interpretation of downstream effects (Figure 5.4, Figure 5.5, Figure 5.6).

GCN2 and PKR inhibition consistently attenuated OTA-induced p-eIF2α in all three cell lines, whereas PERK inhibition had no effect on MEF (Figure 5.9) produced only modest suppression in HK-2 cells (Figure 5.7) and even potentiated p-eIF2α in WB-F344 cells (Figure 5.8), suggesting compensatory ISR signaling upon PERK blockade. Despite similar reductions in p-eIF2α, translational recovery was kinase- and cell-type-specific: GCN2 inhibition partially restored translation in all models, PKR inhibition relieved repression in WB-F344 and MEF cells but not in HK-2 cells, while PERK inhibition only partially restore translation in HK-2. These results underline that p-eIF2α levels alone do not dictate translational output; rather, kinase-specific downstream events and cellular context have significant effects of the modulation of this mechanism. The findings highlight the complex and non-linear nature of translational control under stress and underscore the importance of considering both the phosphorylation status and translational machinery when evaluating ISR dynamics.

Furthermore, although partial recovery in translation was observed with A92 and GSK'414 in HK-2 (Figure 5.10), while with C16 and A92 in WB-F344 (Figure 5.11) and MEF (Figure 5.12), the same conditions significantly exacerbated OTA-induced cell death, dramatically pronounced with prolonged exposure. This paradox suggests that eIF2α phosphorylation may serve a protective role under OTA stress, and its suppression, though temporarily beneficial for translation, may ultimately compromise cell survival by disrupting adaptive mechanisms. It was also evident that even in the absence of OTA, GCN2 inhibition alone decreased cell viability, which was further exacerbated with prolonged inhibition. This aligns with previous findings showing that GCN2 activation is crucial for basal cellular metabolism and balanced protein biogenesis even in the absence of stress, because the prolonged inhibition causes excessive protein synthesis and disrupts metabolic homeostasis (Román-Trufero *et al.*, 2025). Although GCN2 inhibition alone reduced cell viability, the pronounced cytotoxicity under OTA co-treatment indicates that OTA imposes additional stress. This suggests that GCN2 is particularly required to counteract OTA-induced proteotoxic burden, distinguishing the effect from the inhibition toxicity.

Interestingly, GSK'414 in combination with OTA caused marked cell death at 24h, while being non-toxic when used alone in all three cell lines (Figure 5.10, Figure 5.11, Figure 5.12), having limited effect on eIF2α phosphorylation and recovery of translation rate only in HK-2 cell line. This striking toxicity under co-treatment, despite its weak impact on the ISR markers, suggests that PERK may function primarily as a pro-survival factor under OTA-induced stress rather than a central mediator of translational repression, which also explains OTA induced p-PERK levels in the literature (Deng *et al.*, 2023). Its inhibition likely compromises the cell's ability to manage ER stress or oxidative damage triggered by OTA, tipping the balance toward cell death. The findings suggest a cytoprotective role for PERK under prolonged exposure to OTA, potentially downstream of main translation inhibition mechanisms, or independently altogether.

Together, the data indicate that OTA-induced global translation inhibition is predominantly mediated by GCN2 and PKR, with PERK playing a secondary or compensatory role. Furthermore, ISR engagement acts as a double-edged sword, inhibiting protein synthesis while simultaneously supporting survival.

6.2. Cross-talk Between PI3K/Akt/mTOR Signaling and eIF2α Phosphorylation Under OTA Stress

While eIF2α phosphorylation limits global translation under OTA exposure, previous studies have shown that OTA simultaneously activates the PI3K/Akt/mTOR pathway to promote survival, suggesting a contradictory cellular response balancing growth suppression and adaptation. Akt phosphorylation at Ser473 and the activation of mTORC1 downstream targets such as p70 and S6 ribosomal protein were reported to increase in a dose- and time-dependent manner following OTA treatment (Ozcan *et al.*, 2015). This activation may serve as a compensatory mechanism, enabling selective survival and stress adaptation even in the presence of translational arrest. However, whether and how this survival pathway interacts with ISR signaling had not yet been addressed in OTA-related stress studies.

To investigate the relationship between these two responses, the effects of eIF2α kinase inhibition on PI3K/Akt/mTOR activity were examined at 12h of OTA exposure in HK-2 and WB-F344 cells, and at 6h in MEFs, time points that coincided with peak p-eIF2α levels in each cell type (Figure 5.13). Phosphorylation of Akt (Ser473), p70 (Thr389), and S6 (Ser235/236) were evaluated as readouts of pathway activity. Interestingly, inhibition of GCN2 (via A92) and led to a marked reduction in p-Akt levels across all three cell lines, both alone and in combination with OTA, while the same effect was observed with inhibition of PKR (via C16) in WB-F344 and MEF cells, suggesting that ISR kinases, particularly GCN2, contribute to the maintenance of Akt activity under stress conditions along with basal homeostasis. Notably, PERK inhibition (via GSK'414) exerted only a mild or inconsistent effect on Akt phosphorylation, indicating a less significant role in this cross-regulation.

As for the downstream mTORC1 signaling, the pattern was more complex. GCN2 inhibition consistently reduced phosphorylation of both p70 and S6 across all cell types, implicating GCN2 as a key upstream modulator not only of Akt but also of mTORC1 signaling. PKR inhibition had a more variable effect, moderately reducing p70 and S6 in WB-F344 and MEFs but having limited impact in HK-2 cells. Surprisingly, A92 treatment alone caused a notable suppression of p70 and S6 even in the absence of OTA, suggesting a basal contribution of GCN2 activity to mTORC1 signaling homeostasis, independent of stress induction.

To assess the reciprocal direction of this cross-talk, the ISR response was probed under chemical inhibition of the PI3K/Akt/mTOR pathway, in HK-2 (Figure 5.14) and WB-F344 (Figure 5.15) cell lines. PI3K inhibition via wortmannin was confirmed by decreased p-Akt levels and resulted in a significant reduction in p-eIF2α under OTA exposure, particularly at the peak activation time points. This finding was consistent across HK-2 and WB-F344 cells and indicates that PI3K/Akt activity contributes to sustaining ISR signaling during OTA-induced stress. mTORC1 inhibition via rapamycin had no discernible effect on WB-F344 cells but led to a mild attenuation of p-eIF2α in HK-2 cells, despite successful pathway inhibition confirmed by reduced p70

and S6 phosphorylation. This limited response suggests that the PI3K arm, rather than mTORC1 downstream targets, plays a more dominant role in promoting eIF2α phosphorylation in this context.

These findings collectively reveal a functional and bidirectional interplay between eIF2α phosphorylation and PI3K/Akt/mTOR pathways. On one hand, ISR kinases, particularly GCN2, appear to facilitate Akt and mTORC1 activation, potentially supporting the cell's survival strategy under OTA stress. On the other hand, PI3K/Akt signaling promotes eIF2α phosphorylation. This cross-dependence is particularly evident in the fact that inhibition of either pathway alone compromises the cellular response, as reflected by heightened cytotoxicity and disrupted signaling balance.

Taken together, these data emphasize that the cellular response to OTA, particularly the regulation of eIF2α phosphorylation and protein synthesis inhibition, is not governed by a single isolated pathway but emerges through a coordinated and cell-type-specific network of stress and survival signaling. The ISR and PI3K/Akt/mTOR pathways form an interlinked regulatory circuit, wherein modulation of one arm feeds back into the other. Understanding this crosstalk helps explain the underlying mechanisms beyond surface-level observations, shedding light on how cells actively try to maintain balance and survive during OTA stress

Given that inhibition of global protein synthesis is one of the most consistently cited effects of OTA exposure across various biological models, elucidating the molecular mechanisms driving this phenomenon is critical. This study sheds light on the upstream regulation of eIF2α phosphorylation, particularly through GCN2 and PKR, and highlights its functional interplay with the PI3K/Akt/mTOR pathway. These findings suggest that translational repression under OTA stress is not merely a consequence of toxicity, but part of a broader adaptive strategy aimed at maintaining cellular balance. Considering the strong association between OTA exposure and progressive renal pathologies such as CKD and BEN, which lack effective curative options, the mechanistic insights gained here may hold translational relevance. Targeting GCN2 activity

or its downstream translational programs in a temporally controlled and tissue-specific manner could help balance stress adaptation and limit long-term cytotoxic effects of chronic OTA exposure. Furthermore, as translational control is a central component of the cellular stress response in many pathological contexts, the dysregulation caused by OTA may also contribute to toxic outcomes beyond the kidney. Thus, a deeper understanding of these signaling events not only informs OTA-induced nephrotoxicity but may also uncover broader implications in the context of mycotoxin-related diseases.

As future perspectives, the ISR kinases can be specifically knocked-down to identify molecular attributions more clearly, since chemical inhibition might cause unintended effects on cellular responses. Furthermore, the activation of kinases can be visualized via phospho-specific antibodies for further confirmation. This study proposes that the explored mechanism induces an adaptive response under OTA-exposure. Consequently, these adaptive changes can be further investigated using more powerful tools such as ribosome profiling assays.

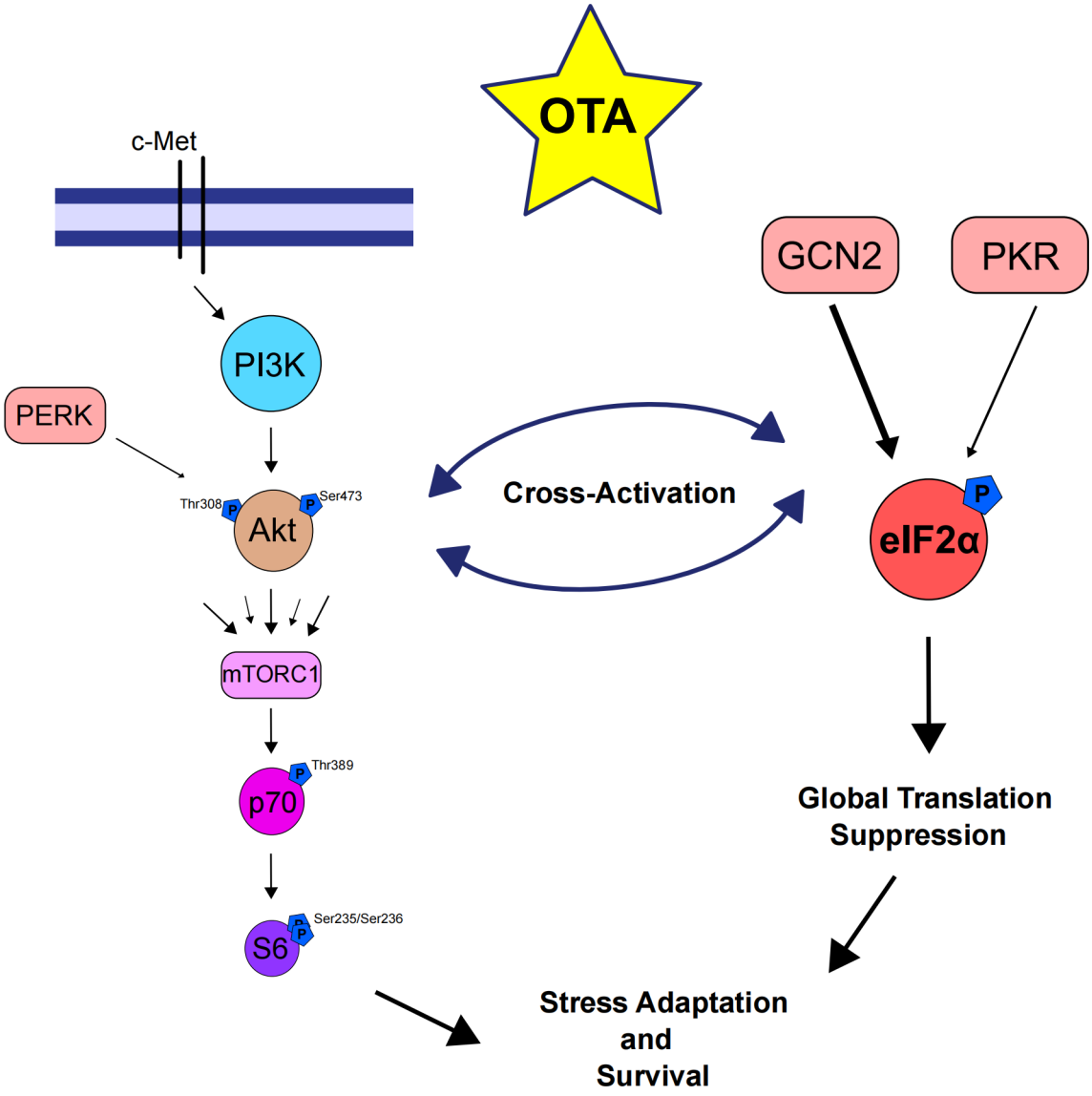

Figure 6.1: OTA activates GCN2 and PKR, causing eIF2α phosphorylation and global translation repression, while also stimulating PI3K/Akt/mTOR and phosphorylation of p70 and S6 (Ozcan et al., 2015). The pathways interact bidirectionally, with ISR kinases supporting Akt/mTORC1 and PI3K/Akt contributing to eIF2α phosphorylation.

REFERENCES

Akpinar, H. A., H. Kahraman, and I. Yaman, 2019, Ochratoxin A Sequentially Activates Autophagy and the Ubiquitin–Proteasome System, *Toxins*, Vol. 11, No. 11, p. 615.

Aviner, R., 2020, The Science of Puromycin: From Studies of Ribosome Function to Applications in Biotechnology, *Computational and Structural Biotechnology Journal*, Vol. 18, pp. 1074–1083.

Bagratuni, T., D. Patseas, N. Mavrianou-Koutsoukou, C. I. Liacos, A. D. Sklirou, P. Rousakis, M. Gavriatopoulou, E. Terpos, O. E. Tsitsilonis, I. P. Trougakos, E. Kastritis, and M. A. Dimopoulos, 2020, Characterization of a PERK Kinase Inhibitor With Anti-Myeloma Activity, *Cancers*, Vol. 12, No. 10, p. 2864.

Brazeau, J. F., and G. Rosse, 2014, Triazolo[4,5-d]pyrimidine Derivatives as Inhibitors of GCN2, *ACS Medicinal Chemistry Letters*, Vol. 5, No. 4, pp. 282–283.

Creppy, E. E., F. C. Stormer, D. Kern, R. Roschenthaler, and G. Dirheimer, 1983, Effects of Ochratoxin A Metabolites on Yeast Phenylalanyl-tRNA Synthetase and on the Growth and In Vivo Protein Synthesis of Hepatoma Cells, *Chemico-Biological Interactions*, Vol. 47, No. 2, pp. 239–247.

Dann, S. G., and G. Thomas, 2006, The Amino Acid Sensitive TOR Pathway From Yeast to Mammals, *FEBS Letters*, Vol. 580, No. 12, pp. 2821–2829.

Deng, H., W. Chen, B. Zhang, Y. Zhang, L. Han, Q. Zhang, S. Yao, H. Wang, and X. L. Shen, 2023, Excessive ER-Phagy Contributes to Ochratoxin A–Induced Apoptosis, *Food and Chemical Toxicology*, Vol. 176, p. 113793.

El Khoury, A., and A. Atoui, 2010, Ochratoxin A: General Overview and Actual Molecular Status, *Toxins*, Vol. 2, No. 4, pp. 461–493.

European Commission, 2006, Commission Regulation (EC) No. 1881/2006 of 19 December 2006 Setting Maximum Levels for Certain Contaminants in Foodstuffs, *Official Journal of the European Union*, L 364, pp. 5–24.

Gekle, M., C. Sauvant, and G. Schwerdt, 2005, Ochratoxin A at Nanomolar Concentrations: A Signal Modulator in Renal Cells, *Molecular Nutrition & Food Research*, Vol. 49, No. 2, pp. 118–130.

Glaviano, A., A. S. C. Foo, H. Y. Lam, K. C. H. Yap, W. Jacot, R. H. Jones, H. Eng, M. G. Nair, P. Makvandi, B. Geoerger, M. H. Kulke, R. D. Baird, J. S. Prabhu, D. Carbone, C. Pecoraro, D. B. L. Teh, G. Sethi, V. Cavalieri, K. H. Lin, and A. P. Kumar, 2023, PI3K/AKT/mTOR Signaling Transduction Pathway and Targeted Therapies in Cancer, *Molecular Cancer*, Vol. 22, No. 1, p. 138.

Haze, K., T. Okada, H. Yoshida, H. Yanagi, T. Yura, M. Negishi, and K. Mori, 2001, Identification of the G13 (cAMP-Response-Element–Binding Protein–Related Protein) Gene Product Related to Activating Transcription Factor 6 as a Transcriptional Activator of the Mammalian Unfolded Protein Response, *The Biochemical Journal*, Vol. 355, pt. 1, pp. 19–28.

Hmaissia Khlifa, K., R. Ghali, C. Mazigh, Z. Aouni, S. Machgoul, and A. Hedhili, 2012, Ochratoxin A Levels in Human Serum and Foods From Nephropathy Patients in Tunisia: Where Are You Now?, *Experimental and Toxicologic Pathology*, Vol. 64, No. 5, pp. 509–512.

Holcik, M., 2015, Could the eIF2α-Independent Translation Be the Achilles' Heel of Cancer?, *Frontiers in Oncology*, Vol. 5, p. 264.

Inoki, K., Y. Li, T. Zhu, J. Wu, and K.-L. Guan, 2002, TSC2 Is Phosphorylated and Inhibited by Akt and Suppresses mTOR Signalling, *Nature Cell Biology*, Vol. 4, No. 9, pp. 648–657.

Isotani, S., K. Hara, C. Tokunaga, H. Inouc, J. Avruch, and K. Yonczawa, 1999, Immunopurified Mammalian Target of Rapamycin Phosphorylates and Activates p70 S6 Kinase Alpha In Vitro, *Journal of Biological Chemistry*, Vol. 274, No. 48, pp. 34493–34498.

Jammi, N. V., L. R. Whitby, and P. A. Beal, 2003, Small Molecule Inhibitors of the RNA-Dependent Protein Kinase, *Biochemical and Biophysical Research Communications*, Vol. 308, No. 1, pp. 50–57.

Jin, H.-O., S.-E. Hong, J.-Y. Kim, S.-K. Jang, and I.-C. Park, 2021, Amino Acid Deprivation Induces AKT Activation by Inducing the GCN2/ATF4/REDD1 Axis, *Cell Death Disease*, Vol. 12, No. 12, p. 1127.

Kalghatgi, S., C. S. Spina, J. C. Costello, M. Liesa, J. R. Morones-Ramirez, S. Slomovic, A. Molina, O. S. Shirihai, and J. J. Collins, 2013, Bactericidal Antibiotics Induce Mitochondrial Dysfunction and Oxidative Damage in Mammalian Cells, *Science Translational Medicine*, Vol. 5, No. 192, p. 192ra85.

Kosicki, R., J. Buharowska-Donten, and M. Twarużek, 2021, Ochratoxin A Levels in Serum of Polish Dialysis Patients With Chronic Renal Failure, *Toxicon*, Vol. 200, pp. 183–188.

Krishnamoorthy, T., G. D. Pavitt, F. Zhang, T. E. Dever, and A. G. Hinnebusch, 2001, Tight Binding of the Phosphorylated Alpha Subunit of Initiation Factor 2 (eIF2α) to the Regulatory Subunits of Guanine Nucleotide Exchange Factor eIF2B Is Required for Inhibition of Translation Initiation, *Molecular and Cellular Biology*, Vol. 21, No. 15, pp. 5018–5030.

Lu, L., A. P. Han, and J. J. Chen, 2001, Translation Initiation Control by Heme-Regulated Eukaryotic Initiation Factor 2α Kinase in Erythroid Cells Under Cytoplasmic Stresses, *Molecular and Cellular Biology*, Vol. 21, No. 23, pp. 7971–7980.

Meucci, V., G. Luci, M. Vanni, G. Guidi, F. Perondi, and L. Intorre, 2017, Serum Levels of Ochratoxin A in Dogs With Chronic Kidney Disease (CKD): A Retrospective Study, *The Journal of Veterinary Medical Science*, Vol. 79, No. 2, pp. 440–447.

Moullan, N., L. Mouchiroud, X. Wang, D. Ryu, E. G. Williams, A. Mottis, V. Jovaisaite, M. V. Frochaux, P. M. Quiros, B. Deplancke, R. H. Houtkooper, and J. Auwerx, 2015, Tetracyclines Disturb Mitochondrial Function Across Eukaryotic Models: A Call for Caution in Biomedical Research, *Cell Reports*, Vol. 10, No. 10, pp. 1681–1691.

Mounir, Z., J. L. Krishnamoorthy, S. Wang, B. Papadopoulou, S. Campbell, W. J. Muller, M. Hatzoglou, and A. E. Koromilas, 2011, Akt Determines Cell Fate Through Inhibition of the PERK–eIF2α Phosphorylation Pathway, *Science Signaling*, Vol. 4, No. 192, p. ra62.

Ozcan, Z., G. Gul, and I. Yaman, 2015, Ochratoxin A Activates Opposing c-MET/PI3K/Akt and MAPK/ERK 1–2 Pathways in Human Proximal Tubule HK-2 Cells, *Archives of Toxicology*, Vol. 89, No. 8, pp. 1313–1327.

Pakos-Zebrucka, K., I. Koryga, K. Mnich, M. Ljujic, A. Samali, and A. M. Gorman, 2016, The Integrated Stress Response, *EMBO Reports*, Vol. 17, No. 10, pp. 1374–1395.

Pavlova, N. N., B. King, R. H. Josselsohn, S. Violante, V. L. Macera, S. A. Vardhana, J. R. Cross, and C. B. Thompson, 2020, Translation in Amino Acid–Poor Environments Is Limited by tRNA,(Gln) Charging, *eLife*, Vol. 9, p. e62307.

Rajesh, K., J. Krishnamoorthy, U. Kazimierczak, C. Tenkerian, A. I. Papadakis, S. Wang, and S. Huang, and A. E. Koromilas, 2015, Phosphorylation of the Translation Initiation Factor eIF2α at Serine 51 Determines the Cell Fate Decisions of Akt in Response to Oxidative Stress, *Cell Death Disease*, Vol. 6, p. e1591.

Román-Trufero, M., I. T. Kleijn, K. Blighe, J. Zhou, P. Saavedra-García, A. Gaffar, M. Christoforou, A. Bellotti, J. Abrahams, A. Atrih, D. Lamont, M. Gierlinski, P. Jayaprakash, A. M. Michel, E. O. Aboagye, M. Yuneva, G. R. Masson, V. Shahrezaei, and H. W. Auner, 2025, An ISR-Independent Role of GCN2 Prevents Excessive Ribosome Biogenesis and mRNA Translation, *Life Science Alliance*, Vol. 8, No. 5, p. e202403014.

Sorrenti, V., C. Di Giacomo, R. Acquaviva, I. Barbagallo, M. Bognanno, and F. Galvano, 2013, Toxicity of Ochratoxin A and Its Modulation by Antioxidants: A Review, *Toxins*, Vol. 5, No. 10, pp. 1742–1766.

Sun, S. S. Y., L. M. Rosenberg, X. Wang, Z. Zhou, P. Yue, H. Fu, and F. R. Khuri, 2005, Activation of Akt and eIF4E Survival Pathways by Rapamycin-Mediated Mammalian Target of Rapamycin Inhibition, *Cancer Research*, Vol. 65, No. 16, pp. 7052–7058.

Szaruga, M., D. A. Janssen, C. de Miguel, G. Hodgson, A. Fatalska, A. P. Pitera, A. Andreeva, and A. Bertolotti, 2023, Activation of the Integrated Stress Response by Inhibitors of Its Kinases, *Nature Communications*, Vol. 14, No. 1, p. 5535.

Torrence, M. E., M. R. MacArthur, A. M. Hosios, A. J. Valvezan, J. M. Asara, J. R. Mitchell, and B. D. Manning, 2021, The mTORC1–Mediated Activation of ATF4 Promotes Protein and Glutathione Synthesis Downstream of Growth Signals, *eLife*, Vol. 10, p. e63326.

Wang, Y., J. Cui, G. Zheng, M. Zhao, Z. Hao, H. Lian, Y. Li, W. Wu, X. Zhang, and J. Wang, 2022, Ochratoxin A Induces Cytotoxicity Through the ROS-Mediated Endoplasmic Reticulum Stress Pathway in Human Gastric Epithelium Cells, *Toxicology*, Vol. 479, p. 153309.

Xu, H., J. Chen, X. Si, M. Chen, F. Pei, C. Qiu, J. Wu, and X. Guan, 2018, PKR Inhibition Mediates Endotoxin Tolerance in Macrophages Through Inactivation of PI3K/AKT Signaling, *Molecular Medicine Reports*, Vol. 18, No. 2, pp. 1999–2006.

Yang, S. A., K. H. Rhee, H. J. Yoo, M. C. Pyo, and K. W. Lee, 2023, Ochratoxin A Induces Endoplasmic Reticulum Stress and Fibrosis in the Kidney via the HIF-1α/miR-155-5p Link, *Toxicology Reports*, Vol. 10, pp. 133–145.

Yerlikaya, A., 2022, Heme-Regulated Inhibitor: An Overlooked eIF2α Kinase in Cancer Investigations, *Medical Oncology*, Vol. 39, No. 7, p. 73.

Yoneyama, Y., T. Inamitsu, K. Chida, S. I. Iemura, T. Natsume, T. Maeda, F. Hakuno, and S. I. Takahashi, 2018, Serine Phosphorylation by mTORC1 Promotes IRS-1 Degradation Through SCFβ-TRCP E3 Ubiquitin Ligase, *iScience*, Vol. 5, pp. 1–18.